AD_____

Award Number: W81XWH-07-1-0387

TITLE: The Role of XMRV, a novel xenotropic murine retrovirus, in human prostate cancer

PRINCIPAL INVESTIGATOR: Stephen P. Goff, PhD; Ila R. Singh, MD, PhD

CONTRACTING ORGANIZATION: Columbia University, New York, NY 10027

REPORT DATE: May 2009

TYPE OF REPORT: Annual Progress report

PREPARED FOR: U.S. Army Medical Research and Materiel Command
Fort Detrick, Maryland 21702-5012

DISTRIBUTION STATEMENT:

X Approved for public release; distribution unlimited

REPORT DOCUMENTATION PAGE

Form Approved
OMB No. 0704-0188

1. REPORT DATE *(DD-MM-YYYY)*	**2. REPORT TYPE**	**3. DATES COVERED** *(From - To)*
01-05-2009	Annual Progress report	23 April 2008 -22 April 2009

4. TITLE AND SUBTITLE
The Role of XMRV, a novel xenotropic murine retrovirus,

in human prostate cancers

5a. CONTRACT NUMBER

5b. GRANT NUMBER
W81XWH-07-1-0387

5c. PROGRAM ELEMENT NUMBER

6. AUTHOR(S)
Stephen Goff, Jason Rodriguez
Ila Singh, Robert Schlaberg, Daniel Choe, Kristy Brown, Harsh Thaker

5d. PROJECT NUMBER

5e. TASK NUMBER

5f. WORK UNIT NUMBER

7. PERFORMING ORGANIZATION NAME(S) AND ADDRESS(ES)
Columbia University

New York, NY 10027

8. PERFORMING ORGANIZATION REPORT NUMBER

9. SPONSORING / MONITORING AGENCY NAME(S) AND ADDRESS(ES)
U.S. Army Medical Research
Materiel Command
Fort Detrick, MD 21702-5012

10. SPONSOR/MONITOR'S ACRONYM(S)

11. SPONSOR/MONITOR'S REPORT NUMBER(S)

12. DISTRIBUTION / AVAILABILITY STATEMENT

Approved for public release; distribution unlimited

13. SUPPLEMENTARY NOTES

14. ABSTRACT Xenotropic murine leukemia virus–related virus (XMRV) was recently discovered in human prostate cancers and is the first gammaretrovirus known to infect humans. While gammaretroviruses have well-characterized oncogenic effects in animals, they have not been shown to cause human cancers. We provide experimental evidence that XMRV is indeed a gammaretrovirus with protein composition and particle ultrastructure highly similar to Moloney murine leukemia virus (MoMLV). We analyzed 334 consecutive prostate resection specimens, using a qPCR assay and immunohistochemistry with an anti-XMRV specific antiserum. We found XMRV DNA in 6% and XMRV protein expression in 23% of prostate cancers. XMRV proteins were expressed in malignant epithelial cells, suggesting that retroviral infection may be directly linked to tumorigenesis. XMRV infection was associated with prostate cancer, especially higher-grade cancers. We found XMRV infection to be independent of a common polymorphism in the *RNASEL* gene, unlike previously reported. This result increases the population at risk for XMRV infection from only those homozygous for the *RNASEL* variant to all individuals. Our observations provide new evidence for an association of XMRV with malignant cells and with more aggressive tumors.

XMRV displayed robust expression and infection in LNCaP prostate tumor cells. The transcriptional activity of the XMRV LTR was found to be higher than the MoMLV LTR in both LNCaP and WPMY-1 cells. The U3 promoter of XMRV and a glucocorticoid response element (GRE) in the U3 were required for transcriptional activity. Co-expression of the androgen receptor and stimulation with androgen stimulated XMRV-LTR dependent transcription in 293T cells and the GRE was required for this activity. Our data suggest that XMRV replicates more efficiently in certain prostate tumor cells in part due to the transcriptional environment in the prostate tumor cells.

15. SUBJECT TERMS
XMRV, retrovirus, malignant epithelium, qPCR, immunohistochemistry, long terminal repeat, LTR, transcription, luciferase

16. SECURITY CLASSIFICATION OF:			**17. LIMITATION OF ABSTRACT**	**18. NUMBER OF PAGES**	**19a. NAME OF RESPONSIBLE PERSON**
a. REPORT	**b. ABSTRACT**	**c. THIS PAGE**			USAMRMC
U	U	U	UU	55	**19b. TELEPHONE NUMBER** *(include area code)*

Table of Contents

Page

The Role of XMRV, a Novel Xenotropic Murine Retrovirus, in Human Prostate Cancers

Stephen P. Goff and Ila Singh, co-PIs

INTRODUCTION

Xenotropic murine leukemia virus–related virus (XMRV) was recently discovered in human prostate cancers [1] and is the first gammaretrovirus known to infect humans. While gammaretroviruses have well-characterized oncogenic effects in animals, they have not been shown to cause human cancers. We provide experimental evidence that XMRV is indeed a gammaretrovirus with protein composition and particle ultrastructure highly similar to Moloney murine leukemia virus (MoMLV). We analyzed 334 consecutive prostate resection specimens, using a qPCR assay and immunohistochemistry with an anti-XMRV specific antiserum. We found XMRV DNA in 6% and XMRV protein expression in 23% of prostate cancers. XMRV proteins were expressed in malignant epithelial cells, suggesting that retroviral infection may be directly linked to tumorigenesis. XMRV infection was associated with prostate cancer, especially higher-grade cancers. We found XMRV infection to be independent of a common polymorphism in the RNASEL gene, unlike previously reported. This result increases the population at risk for XMRV infection from only those homozygous for the RNASEL variant to all individuals. Our observations provide new evidence for an association of XMRV with malignant cells and with more aggressive tumors [2].

XMRV displayed robust expression and infection in LNCaP prostate tumor cells. The transcriptional activity of the XMRV LTR was found to be higher than the MoMLV LTR in both LNCaP and WPMY-1 cells. The U3 promoter of XMRV and a glucocorticoid response element (GRE) in the U3 were required for transcriptional activity. Co-expression of the androgen receptor and stimulation with androgen stimulated XMRV-LTR dependent transcription in 293T cells and the GRE was required for this activity. Our data suggest that XMRV replicates more efficiently in certain prostate tumor cells in part due to the transcriptional environment in the prostate tumor cells [3].

BODY

Our specific aims remain unchanged. Our progress towards them is reported below.

Aim 1: Construction of an infectious proviral DNA clone of XMRV and characterization of its replication in cell culture.

XMRV was recently discovered [1] in prostate cancer tissues from men homozygous for a reduced activity variant of an antiviral gene, RNASEL. Two overlapping partial cDNAs of XMRV derived from human prostate cancer tissue [1], were obtained as a gift from the Ganem laboratory. In our laboratories, we joined the two genomic halves AM 2-9 and AO H4 by introducing a novel MluI site and performing overlapping PCR (Fig. 1). This MluI restriction site generated a single amino acid change: glycine to alanine at position 385 of reverse transcriptase. This full-length clone was infectious (see below), and its sequence was similar to that in the original report. However, this genomic clone lacked a 5'-U3 region, which normally harbors promoter activity and a functional TATA box. In its absence, it would be difficult to get maximal transcription. Thus, to generate the provirus the U3 region was amplified and fused to the 5' LTR using traditional PCR techniques

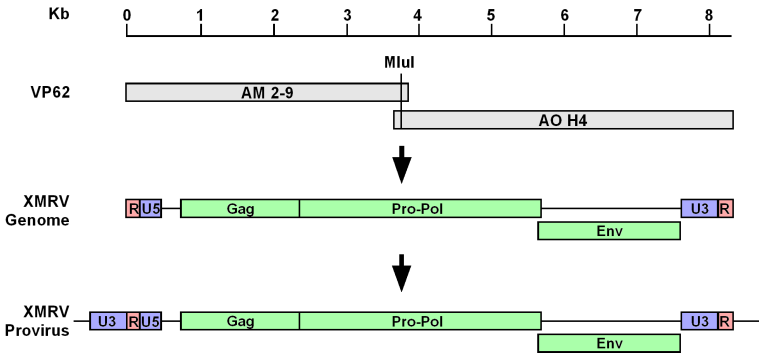

Fig. 1: Construction of XMRV provirus. Two halves of XMRV from prostate cancer patient VP62 were joined by introducing an MluI restriction site and performing overlapping PCR. The provirus was created by fusing the U3 promoter to the 5' LTR region. The provirus was ligated to a mammalian expression vector.

Introducing this proviral DNA into 293T cells resulted in release of viral particles several days after transfection, as seen by reverse transcriptase activity in the supernatants. Naïve 293T cells were inoculated with this culture supernatant, and the cells serially passaged, resulting in chronically infected 293T cells. Infected cells as well as released particles were analyzed by transmission electron microscopy (Fig. 2). Particles of approximately 120 nm diameters, with

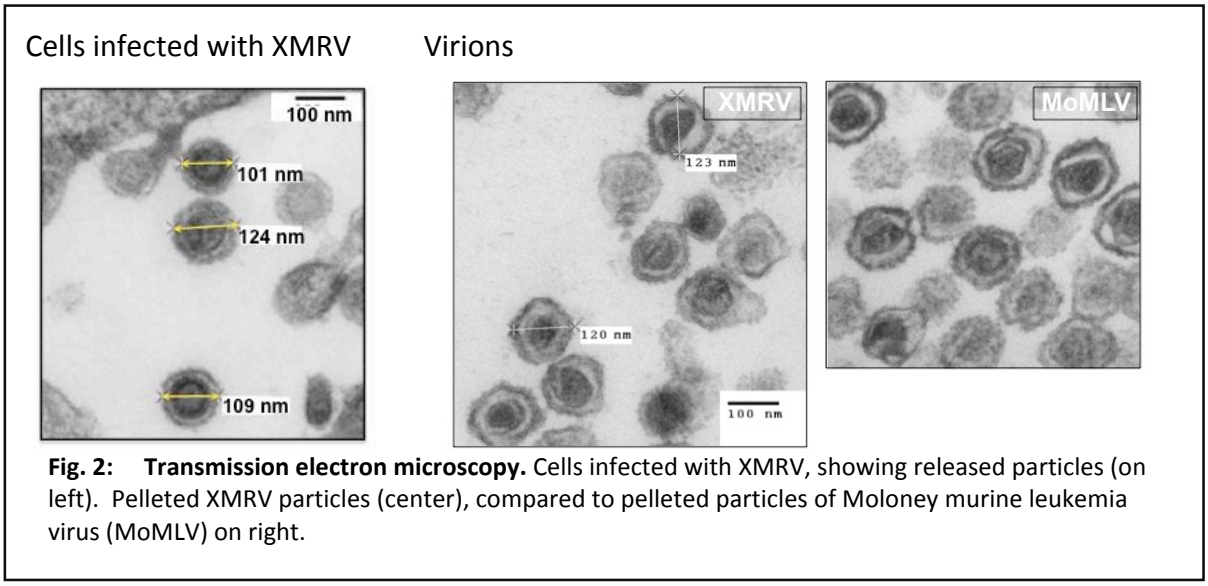

Fig. 2: Transmission electron microscopy. Cells infected with XMRV, showing released particles (on left). Pelleted XMRV particles (center), compared to pelleted particles of Moloney murine leukemia virus (MoMLV) on right.

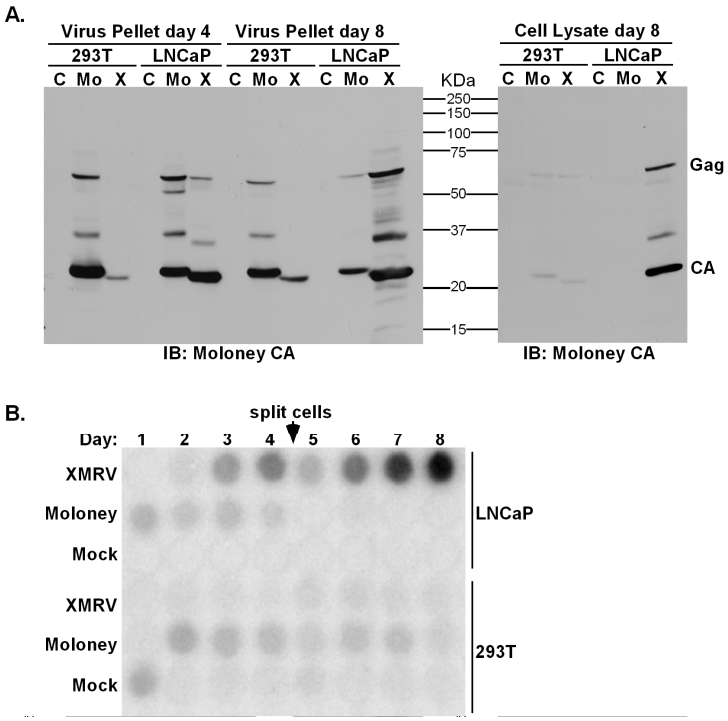

Fig. 3: Production of XMRV viral particles from LNCaP cells. (A) LNCaP and 293T cells were transfected with XMRV and Moloney proviral constructs and viral particles in the media were pelleted by ultracentrifugation and lysed 4 and 8 days post-transfection *(Left)*. XMRV transfected cells were also lysed on day 13 *(Right)*. Proteins were separated by SDS-PAGE and analyzed by immunoblotting with Moloney MLV CA antisera (sufficient homology exists for cross-reactivity). C - Mock control; Mo – Moloney MLV; X – XMRV. (B) RT activity released into the media was detected as described in (5). Cells were split on the fourth day and samples taken until day 8.

morphology typical of type C retroviruses were seen. An electron micrograph of Moloney murine leukemia virus (MoMLV), a prototypic type C retrovirus is shown alongside for comparison.

Aim 2: Testing and mapping determinants of XMRV pathogenicity; generation of mouse models susceptible to XMRV infection;

Numerous cell lines were tested for viral protein expression and for subsequent release of virus particles. 293T (human embryonic kidney), 2fTGH (human fibrosarcoma), HeLa (cervical carcinoma), and TE671 (rhabdomyosarcoma) produced XMRV virus particles but the titers were low (data not shown). 293T cells and LNCaP cells were transfected with the provirus and monitored for the intracellular expression of XMRV gene products and the accumulation of virus particles in cell culture supernatants (Fig. 3). Four and eight days post-transfection, viral proteins of both Moloney MLV (MoMLV) and XMRV were detected in the media. 293T cell supernatants contained a very small amount of XMRV viral capsid compared to the MoMLV control. In contrast, XMRV virus protein accumulation was much higher and the same as MoMLV virus particles in LNCaP cells. Over time, XMRV protein accumulated to higher degree than MoMLV consistent with the fact that MLVs cannot spread infection in human cells. Significantly, more XMRV protein was observed in LNCaP cells than in 293T at both time points (Fig. 3A). Cell lysates prepared at day eight of the experiment clearly show unprocessed Gag protein and the capsid (CA) cleavage product of XMRV accumulating to high levels in prostate LNCaP cells but not 293T cells. Functional RT activity was also detected in the media of LNCaP cells suggesting that significant numbers of viral particles were being produced only from LNCaP cells (Fig. 3B).

Next it was determined whether XMRV virus particles produced from LNCaP cells are infectious. Non-infected 293T and LNCaP cells were exposed to LNCaP cell culture supernatants to allow XMRV to adsorb. After replacing the media, RT activity of the cell culture supernatants was measured on consecutive days to monitor release of viral particles (Fig. 4). RT activity was detected in the LNCaP but not 293T cell supernatant indicating that XMRV is conducting a spreading infection more efficiently in prostate cells.

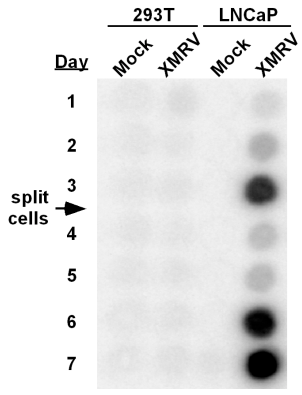

Fig. 4: XMRV spreads infection most efficiently in prostate carcinoma LNCaP cells. Media from LNCaP cells that contained virus particles was passed through a 0.45 μM filter to remove any contaminating cellular debris, and adsorbed onto non-infected cells for two hours with 8 μg/ml of Polybrene. Samples were taken for seven days and assayed for RT activity released into the media. Mock: uninfected control.

The ability of XMRV to perform a spreading infection in three additional cell lines was tested next. XMRV supernatants from LNCaP cells were applied to HeLa (human cervical carcinoma), TE671 (human rhabdomyosarcoma), 2fTGH cells (human fibrosarcoma), and monitored for RT release for three days post-infection (Fig. 5). Only prostate LNCaP cells efficiently supported a spreading infection, suggesting cell-type specificity for XMRV replication.

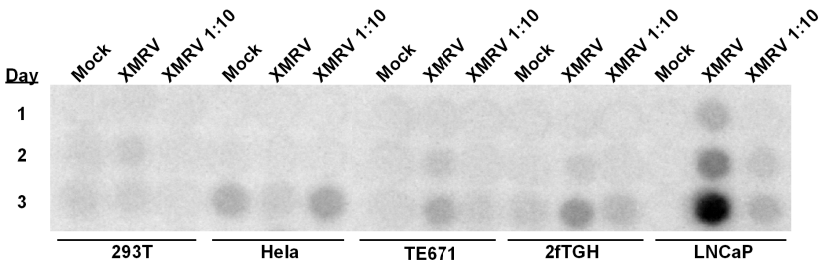

Fig. 5: XMRV spreads infection most efficiently in prostate carcinoma LNCaP cells. Media from LNCaP cells that contained virus particles was passed through a 0.45 μM filter to remove any contaminating cellular debris, and adsorbed onto non-infected cells for two hours with 8 μg/ml of Polybrene. Samples were taken for three days and assayed for RT activity released into the media (5). Mock: uninfected control. XMRV 1:10: XMRV virus stock diluted ten-fold. 293T – human embryonic kidney origin; HeLa – cervical carcinoma; TE671 – human rhabdomyosarcoma; 2fTGH – human fibrosarcoma; LNCaP – human prostate carcinoma.

Multiple hypotheses can explain why XMRV replicates and spreads better in human prostate cells compared to cells of other tissues. First, it is possible that prostate cells may express the cellular receptor while other cell types do not. Expression of XPR1 in prostate cells may confer an entry advantage over other cell types that do not express XPR1, or express the receptor at very low levels. Second, RNase L is thought to be a XMRV restriction factor since most of XMRV-positive tumor samples contained a slightly inactivating mutation in the RNase L gene, HPC1. Some prostate cells lines may indeed have this mutation. Although both theories merit further research, we decided to focus on a third mechanism, namely that prostate cells provide a much more favorable transcriptional environment than other cell types. This would potentially allow for increased viral protein expression and viral release cell culture supernatants.

To test this hypothesis, the 5' LTR of the integrated proviruses from both MoMLV and XMRV up to the Gag expression start site were fused with the luciferase gene. This expression vector can then test the transcriptional output of both MoMLV and XMRV LTRs once they were transfected into different cell types. We also generated a series of 5' and 3' deletions to assign specificity to the transcriptional output (Fig. 6)

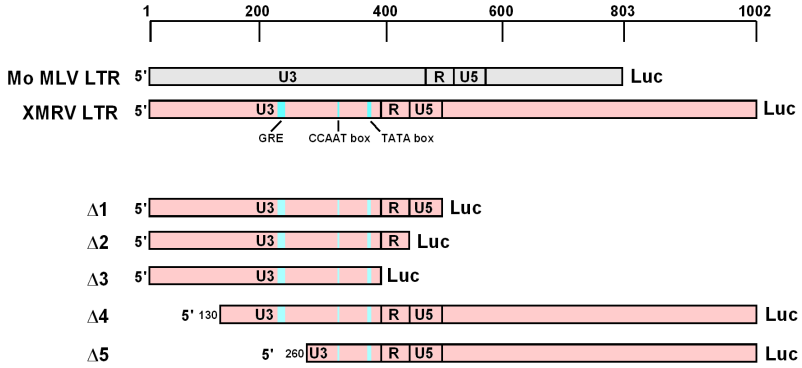

Fig. 6: MoMLV and XMRV LTR-luciferase fusion constructs.
Both MoMLV and XMRV 5' LTRs were amplified by PCR and fused to luciferase in the pRL-null plasmid through sequence and ligation-independent cloning (SLIC). Figures are drawn to scale and the position where truncations were generated are indicated. GRE: Glucocorticoid response element; R: retroviral repeat region.

The expression vectors in Fig. 6 were initially transfected into LNCaP cells to test their transcriptional activity (Fig. 7). A luciferase expression vector without any promoter (Null) and Herpes Simplex virus thymidine kinase (TK) promoter was used as negative and positive controls, respectively. Interestingly the XMRV LTR had much higher (approximately six-fold) transcriptional activity than MoMLV in LNCaP prostate cells. This activity decreased by half when the R, U5, and the untranslated regions were deleted individually. However, any deletion of within the 5' region of U3 dramatically inhibited the

transcriptional activity of XMRV.

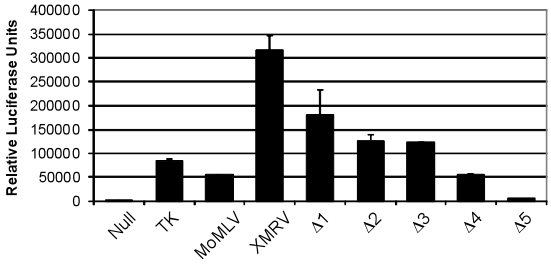

Fig. 7: Transcriptional activity of MoMLV and XMRV LTR-luciferase constructs.
Expression constructs were transfected into LNCaP cells and samples were lysed and analyzed for luciferase activity 24 hours post-transfection. Triplicate samples were co-transfected and normalized to renilla luciferase.

The transcriptional activity of XMRV was higher than MoMLV in LNCaP prostate cells and may be a significant factor in determining cell-type specificity for XMRV protein expression and viral particle accumulation. To confirm this phenomenon, we transfected the LTR-luciferase fusion reporters into 293T, LNCaP and YPMY-1 cells and quantified their transcriptional output (Fig. 8). Significantly, MoMLV activity was higher than XMRV in 293T cells but was lower than XMRV in both LNCaP and YPMY-1 cells. This suggests that XMRV viral particle production depends on the transcriptional environment provided by prostate cells.

Data suggests that the U3 region of the XMRV LTR plays a critical role in transcriptional activation in LNCaP cells. Indeed the U3 region of retrovirus harbors numerous transcription factor-binding sites as well as a functional TATA box for transcription initiation. These response elements vary between different retroviruses and various cell types may exert differential transcriptional activation depending on which factor is expressed. To determine whether the XMRV U3 is necessary and sufficient for transcription in LNCaP cells, a chimeric fusion construct between MoMLV and XMRV were created and fused to luciferase (Fig. 8). This reporter has the XMRV U3 fused to the R, U5 and untranslated region of MoMLV. This, along with MoMLV and XMRV controls, were then transfected into 293T, YMPY-1, or LNCaP cells and analyzed for luciferase activity. As expected, the XMRV transcriptional activity was higher in prostate cells compared to 293T cells. Importantly, the reporter that only contained the XMRV U3 was phenotypically similar to XMRV indicating that the U3 is responsible for the observed differences between non-prostate and prostate cells.

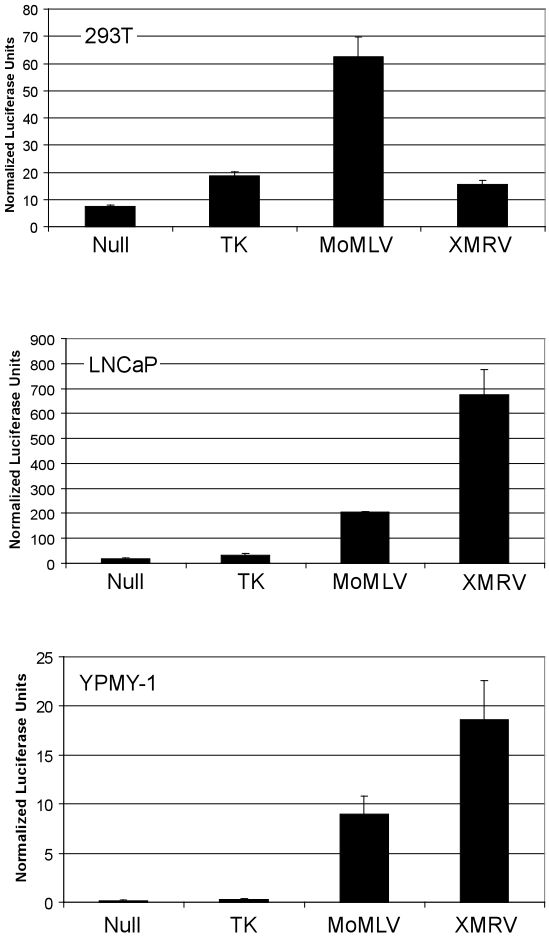

Fig. 8: Transcriptional activity of MoMLV and XMRV in prostate and non-prostate cells. Exactly as described in Fig. 7 except 3 cell lines were used: 293T, LNCaP, and YPMY-1 cells.

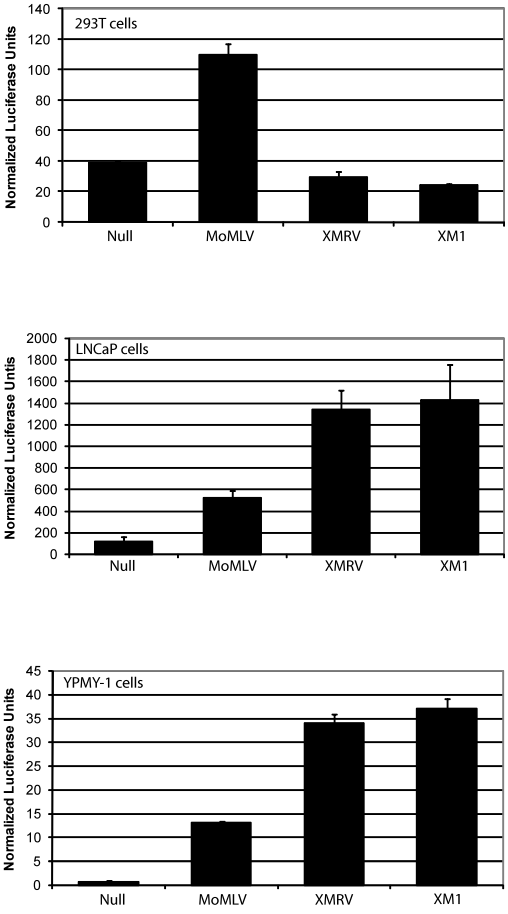

Fig. 9: The U3 region of the XMRV LTR is required for transcriptional activity in prostate cells. Exactly as described in Fig. 7 and using three cell lines, 293T, LNCaP, and YPMY-1 cells. XM1 is a fusion of the XMRV U3 to the R, U5 and untranslated region of MoMLV LTR. This was then fused to the luciferase gene at the ATG start site for MoMLV Gag using SLIC.

Aim 3: Examine human prostate biopsies for XMRV, and for XMRV protein expression

To examine human infection with XMRV in greater depth, we made use of the extensive tissue repositories in the Department of Pathology at Columbia University Medical Center, New York. To estimate the prevalence of XMRV in men with and without prostate cancer, we selected 233 consecutive cases of prostate cancer. For controls, we used 101 consecutive cases of transurethral resection of the prostate for urinary obstruction (most often due to benign prostatic hyperplasia). We also developed several novel tools that allowed us to perform this analysis: a specific quantitative PCR assay (qPCR) described below, highly-specific anti-XMRV antibodies and protocols for immunohistochemistry that allowed for sensitive detection of XMRV proteins in cancers.

Quantitative PCR detection of XMRV proviral DNA

The original report on XMRV identification used an RT-PCR assay to detect XMRV RNA in frozen biopsy tissues. Their nested PCR assay sequentially amplified 612 and 413 nucleotides from the XMRV Gag region of the genome. Since we wished to analyze formalin-fixed paraffin embedded (FFPE) tissues in addition to frozen tissues, it was important that we amplified DNA, and that these amplified DNA segments be as short as possible, both desirable features when working with formalin-fixed tissues. Our qPCR assay employed a fluorescent-labeled Taqman probe containing a minor groove binder/non-fluorescent quencher, flanked by two primers to amplify two regions of the XMRV proviral DNA, 122 bp and 102 bp in length. For primer and probe design, we wanted to select a region in the XMRV proviral DNA that would allow for efficient detection of XMRV without interference from related murine retroviral sequences. Systematic scanning of the entire genome identified a region of the XMRV putative *gag* gene that was 100% conserved between all published XMRV clones (total of 3), and yet shared at most 80% similarity with the most closely related 11 murine retroviral sequences. To further maximize specificity, primers were selected in areas that allowed for greatest mismatch near the 3'-end, and the probe was selected for greatest mismatch at the 5'-end. We used a common forward primer and a common probe in conjunction with two different reverse primers to allow for possible sequence differences in various clinical isolates.

We wanted to ensure that our assay specifically amplified XMRV sequences and not other murine or human endogenous retroviral sequences. In the University tissue repository setting, human tissue blocks, both frozen and paraffin-embedded, are often sectioned on the same microtomes used for murine tissues. Exogenous and endogenous murine retroviruses with high sequence similarity to XMRV are present in multiple copies in the mouse genome and contamination with murine tissues may result in non-specific amplification. To test for amplification of murine ERVs, we used genomic DNA of a C57BL/6 mouse as template. To rule out amplification of human ERVs or possible human sequences related to XMRV, we tested commercially available human placental DNA as template. We also mixed mouse DNA with human placental DNA at different ratios. No amplification product was observed in any of the reactions (data not shown), showing that the qPCR assay was highly specific for XMRV.

We tested sensitivity of our qPCR assay in 2 ways. First, we used serial 10-fold dilutions of plasmid pXMRV33 in 20 ng/µl human placental DNA as template. We could consistently amplify 50 copies of XMRV DNA per reaction each time (Figure 10A). When only 5 copies of XMRV DNA were present per reaction, a detectable amplification product was seen approximately half the times. Our second method assessed sensitivity of amplification from formalin-fixed, paraffin-embedded tissue, using a protocol similar to that used with human prostate tissues. XMRV-infected and naïve 293T cells were mixed together in different ratios: from 1:100 to 1:106 (infected cells: naïve 293T cells). These mixtures of cells were fixed with formalin, embedded in paraffin and sectioned. One of these sections was mixed with nine sections of normal prostate tissue, allowing for a close match between this template DNA and our study material. DNA was extracted and used as template in our qPCR assay (fixed tissue standards). As expected, DNA extracted from naïve 293T cells (mixed with normal prostate) did not result in detectable amplification. XMRV proviral DNA was consistently amplified in up to 1 in 105 dilutions of infected cells (further mixed at approximately 1:10 ratio with normal prostate tissue). One of two duplicates of a 1 in 106 dilution resulted in detectable amplification (Figure 10B). We were thus able to consistently detect low-levels of XMRV-infected cells in our samples, making this a fairly sensitive qPCR assay.

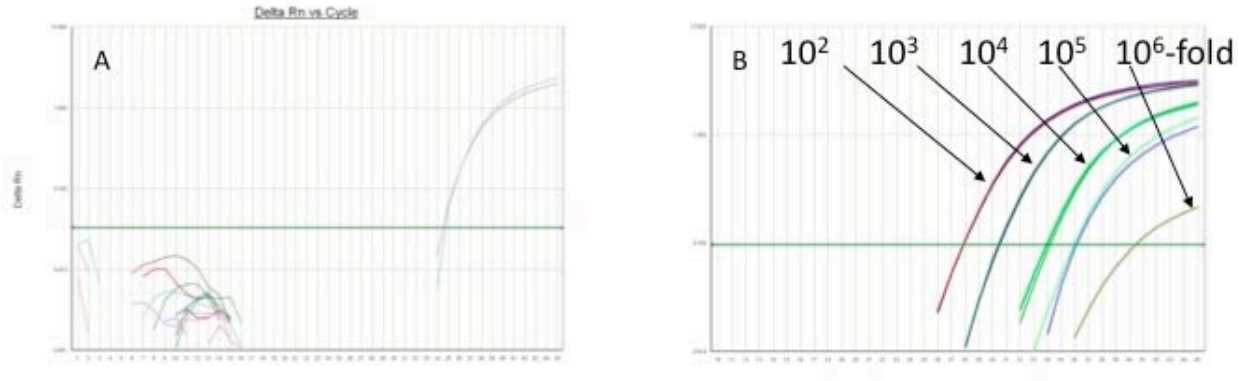

Fig. 10: Developing a sensitive quantitative PCR for detection of XMRV DNA. (A) Amplification of varying amounts of XMRV DNA added to fixed amounts of human placental DNA. Efficient and consistent amplification is seen when at least 50 copies of XMRV genome are present in the reaction. (B) XMRV-infected cells are mixed with uninfected cells at different ratios (1 in 10^2 to 1 in 10^6), fixed in formalin, embedded in paraffin, and then sectioned. One such section is mixed with 9 sections of human prostatic tissue, and DNA is prepared from the mixture. XMRV is efficiently detected in the sample that has 1 infected cell in 10^5, further diluted at least 10 fold in prostate tissue.

DNA extracted from clinical tissues, whether frozen or fixed, can vary in quality depending on processing and storage times and conditions. To test for DNA integrity and the absence of inhibitors of DNA amplification, we developed a second qPCR assay amplifying a 168 bp segment of the human single copy gene, VAMP2. Each of the DNA samples we prepared from prostate tissues was subjected to this VAMP2 qPCR. Amplification product was detectable from all samples: frozen and fixed, ensuring that any failure to detect XMRV was not a result of poor DNA quality in the sample.

Prevalence of XMRV DNA in human prostate tissue

To estimate the prevalence of XMRV in men, 334 consecutive cases of prostatic disease were selected (233 cases of prostate cancer and 101 control cases where prostatic tissues were removed for diagnoses other than cancer). These were men who presented for surgery at Columbia University Medical Center. This analysis is currently ongoing. In brief, XMRV DNA was identified in 11 out of 146 (7.5%) prostate cancers and from 1 in 50 (2.0%) of the control group. The source of tissue in all the control samples was from transurethral resection of the prostate, usually performed with a cauterizing knife, thus making tissue morphology very difficult to analyze. It is impossible to be certain that the control group did not have a small focus of cancer somewhere in the prostate. We are certain, however, that there was no significant difference in DNA quality between these two groups, as determined by amplification of the VAMP2 gene (mean C_T were 25 vs. 24.9 for frozen tissues, 26.4 vs. 25.6 for fixed tissues, and 26.3 vs. 25.3 for fixed control samples respectively).

When FFPE tissue was used as a source of DNA, XMRV was detected in only 3 out of 96 individuals (3.1%) with prostate cancer, in comparison with 11 out of 146 individuals (7.5%) when frozen tissue was tested. This is not unexpected, as PCR amplification of template DNA that has been fixed with formalin and extracted with xylene and other solvents, is known to be poorer than fresh frozen DNA. Furthermore, we found significant sampling differences: analysis of sections from different regions of the prostate, both by PCR and by immunohistochemistry, do not always lead to identical results. In several cases only one of the two duplicate qPCR reactions resulted in detectable amplification products. Low viral loads or polymorphisms in the primer binding sites are possible explanations.

Immunohistochemistry of prostatic tissues for XMRV protein expression

XMRV proteins have previously been reported to be present exclusively in prostatic stromal cells that are near malignant epithelial cells, but never within the cancerous cells themselves. Since all known oncogenic retroviruses transform their host cells directly, new mechanisms need to be invoked if only non-malignant cells harbor the virus. What cell type serves as host for XMRV replication in human prostate cancer tissues, therefore, has significant implications in understanding potential oncogenic mechanisms. In order to carefully address this question, we first generated antisera specific to XMRV. Using these antisera, we then developed an immunohistochemistry (IHC) protocol to determine which cell type expressed XMRV proteins in the prostate cancer tissues used in our study.

We initially used cultured 293T cells that were chronically infected with XMRV for the development and optimization of an XMRV-specific IHC assay. Chronically XMRV-infected 293T cells were fixed with formalin, embedded in paraffin, and the resulting cellblocks sectioned at the same thickness commonly used for IHC analysis of human tissues. Sections were prepared from chronically infected 293T cells (100% infected cells) and serial dilutions of chronically infected 293T cells in naïve 293T cells were made, each containing between 1% to 0.0001% infected cells. We observed strong staining at primary antibody dilutions of 1:7,500 in sections containing 100% infected cells. More than 90% of cells showed granular cytoplasmic staining of varying intensity (Figure 11A). Sections were counterstained with hematoxylin resulting in a blue to purple nuclear staining. As expected, in sections containing 1% infected 293T cells and 99% of naïve cells, only a small subset of cells (approximately 1%) stained positive for XMRV (Figure 11B). As expected, we did not identify any IHC-positive cells in sections containing 100% naïve 293T cells (Figure 11C). We also used pre-immune serum from the same rabbit on all sections stained with specific serum: no staining was seen, as expected (Figure 11D, 11E and 11F). It was thus very likely that using our antisera and IHC protocol, we would be able to specifically visualize XMRV proteins in prostatic tissue.

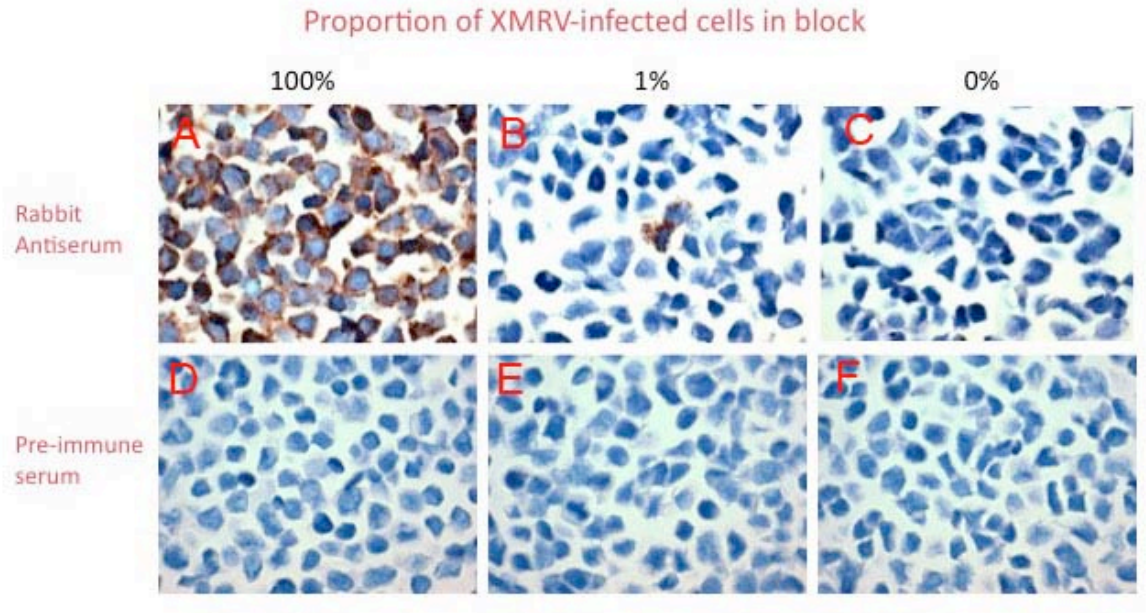

Fig. 11: Immunohistochemistry of XMRV- infected 293T cells (A) 100% XMRV infected cells, (B) 1% XMRV infected cells and (C) uninfected 293T cells were all fixed with formalin, embedded in paraffin to mimic processing of prostate tissues. The blocks were sectioned and stained with anti-XMRV antisera. (D), (E) and (F) are sections corresponding to (A), (B) and (C) that were stained with pre-immune serum from the same rabbit.

However, a protocol developed for immunohistochemical staining of cultured XMRV-infected cells may need further optimization to be used for staining of human prostate tissues. In contrast to sections of infected 293T cells, sections of human prostate tissues contain multiple cell types, varying amounts of fibrous stroma and are not typically processed in a uniform manner. All of this may result in increased background staining. Since no well-defined positive control tissues were available, we first tested sections from cases that were positive by XMRV qPCR. We used conditions optimized for sections of XMRV-infected 293T cells and identified one XMRV qPCR-positive case that showed particularly strong staining of a subset of malignant epithelial cells (Figure 12). At the cellular level, the staining had an identical pattern to that seen in XMRV-infected 293T cells (Figure 11A). We used this case in further analyses to test the observed staining for specificity and further optimize the IHC protocol for use with human prostate tissue sections.

We showed that anti-XMRV antisera from two different rabbits recognized the same clusters of malignant epithelial cells with the same intracellular staining pattern (Figure 12, top row). This staining pattern was identical to that seen in XMRV-infected 293T cells. Pre-absorption of anti-XMRV antiserum did not reduce staining intensity while replacing the anti-XMRV antiserum with pre-immune serum from the same rabbit completely abolished any staining (Figure 12, middle row). We used tissue sections from this case to further optimize antigen retrieval methods, to test varying dilutions and staining parameters of the two anti-XMRV antisera. The protocol resulting in the strongest staining with the least amount of faint, diffuse non-specific staining was used for further analyses of our cases.

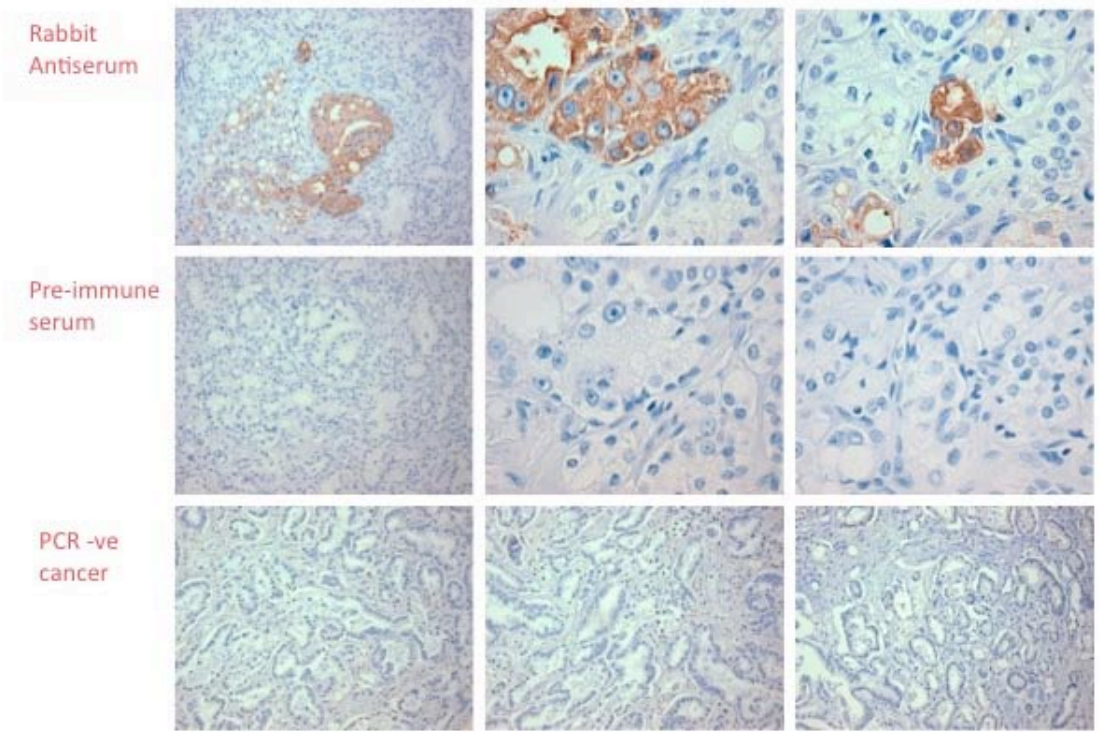

Fig. 12: Immunohistochemistry of Prostate cancers. Human prostate cancers were sectioned and stained with anti-XMRV antisera to look for XMRV protein expression. Top row shows specific staining of malignant epithelial cells. Staining extends to several cells in the same acinus and to cells in the adjacent acini. Stromal cells do not exhibit staining here. Middle row shows adjacent sections stained with pre-immune serum from the same rabbit (notice the identical outline of cells in the top and middle row). Bottom row shows a different case stained with anti-XMRV antisera. This case was negative for XMRV by qPCR and does not show any staining in malignant epithelial cells.

Prevalence and distribution of XMRV protein in human prostate tissue

The human prostate is composed primarily of acinar or ductal epithelial cells, which serve the secretory function of the gland. Almost all cases of human prostate cancer are the result of malignant proliferation of these epithelial cells. In addition to the epithelial cells, the prostate also contains stromal cells, primarily fibroblasts, with a few macrophages, lymphocytes and an occasional granulocyte. To render a pathologic diagnosis of cancer, the entire prostate gland is routinely sampled, resulting in an average of 20-30 tissue blocks that are eventually banked in the tissue repository. Prostate cancer usually follows a focal pattern, with malignant cells seen in only a minority of the sampled tissue blocks. Within each block, the extent of cancer also varies greatly. We examined sections stained with hematoxylin and eosin dyes that were prepared from each block for routine diagnostic purposes. For each case, we selected one or two tissue blocks that contained the highest proportion of malignant epithelial cells for IHC analysis. For every case that showed any staining with IHC, we also tested adjacent sections with control pre-immune serum. With rare exceptions, staining was considered specific if it showed a intracellular pattern similar to that seen in XMRV-infected 293T cells and in the IHC-positive test case shown in Figure 12, without any staining with the pre-immune control serum.

We applied our optimized IHC protocol to prostate tissue sections. In brief, XMRV proteins were expressed in prostatic tissues from 23% with prostate cancer and in 4% without prostate cancer. Interestingly, and in contrast to previous reports, staining was predominantly observed in malignant epithelial cells. Of the IHC-positive cases with prostate cancer, expression of XMRV protein was observed in epithelial cells in 85% of cases, in both epithelial and stromal cells in 7.5% of cases, and exclusively in stromal cells in another 7.5% cases.

Epithelial cells expressing XMRV protein were usually seen clustered in an acinus or in a few acini adjacent to each other (Figure 12, top row). The proportion of cells expressing XMRV protein in a given tissue section varied widely from case to case. However, in all cases the positively staining cells represented the minority of cells in the section. Staining intensity also varied between cases ranging from intense staining of the entire cytoplasm to more discrete staining in which case the granular nature of the staining could be more readily appreciated. The vast majority of IHC-positive epithelial cells showed the same granular staining pattern of the entire cytoplasm described above. In a small number of cases we observed epithelial staining of only a circumscribed portion of the cytoplasm. Rare scattered XMRV-expressing stromal cells were seen in proximity to malignant acini or in lymphocytic infiltrates adjacent to malignant acini. Over all, the number of stromal cells expressing XMRV protein was much smaller than the number of IHC-positive epithelial cells (data not shown).

In summary, we observed expression of XMRV protein in 23% of prostate cancer cases and in only 4% of control cases. We identified XMRV protein most frequently in clusters of epithelial cells that were part of the cancer. Rare stromal cells expressing XMRV protein showed a staining pattern similar to that reported previously. The odds for XMRV being detected in prostate tissues from men with prostate cancer was more than 5 times higher than those for XMRV being present in tissue samples from men without prostate cancer (OR = 5.7, $p \ll 0.001$). We therefore identified a strong correlation between the presence of XMRV DNA and prostate cancer in our study population, using qPCR and XMRV-specific IHC assays for detection of XMRV DNA and protein, respectively. An analysis of tumor samples to show the relationship of the virally infected cells to tumor morphology, grade and stage is in progress.

KEY RESEARCH ACCOMPLISHMENTS

1. We constructed an infectious clone of XMRV, which produced infectious virions when transfected into cells.
2. When analyzed by transmission electron microscopy, XMRV virions produced in cell culture resembled other type-C retroviruses in morphology.
3. The infectious clone of XMRV replicated in human cell lines such as 293Ts, but was especially efficient at replication in prostate cancer cell lines such as LNCaP cells.
4. Transcriptional activity of XMRV was higher than MoMLV in LNCaP prostate cells and may be a significant factor in determining cell-type specificity for XMRV protein expression and viral particle accumulation.
5. Deletion analysis suggested that the U3 region of the XMRV LTR might play a critical role in transcriptional activation in LNCaP cells.
6. We designed a sensitive and specific quantitative PCR assay to detect XMRV DNA from frozen or formalin-fixed, paraffin-embedded prostate tumors.
7. XMRV was found by qPCR in 7.5 % of cancers and 2% of control tissues in our analysis of 146 prostate cancer tissues and 50 control prostate tissues.
8. We generated antisera that are highly specific for XMRV.
9. We designed an immunohistochemistry protocol that specifically detects XMRV protein expression in prostate cancers.
10. XMRV proteins are expressed mostly in malignant epithelial cells. Benign cells do not express XMRV proteins and very rarely do stromal cells express XMRV proteins. This has implications for possible mechanisms of tumorigenesis by XMRV.

REPORTABLE OUTCOMES

1. XMRV resembles other gammaretroviruses in protein composition and morphology
2. An infectious clone of XMRV was generated, that replicates robustly in culture
3. U3 region of XMRV LTR, and specifically the Androgen response element within it play a significant role in determining cell type specificity for XMRV replication.
4. XMRV is present in over a fourth of prostate cancers and in only 6% of benign prostates
5. XMRV proteins are expressed mostly in malignant epithelial cells, consistent with a retroviral model for oncogenesis.
6. XMRV infection does not correlate with the previously reported R482Q mutation in *RNASEL.*
7. Tumors of higher grade are more likely to contain XMRV.

CONCLUSION

XMRV is a recently discovered retrovirus. Our findings suggest a strong association between XMRV and prostate cancer. We find the virus in malignant cells in the prostate and especially in more aggressive or higher grade tumors. The specificity of XMRV replication in prostate cells might be explained by the androgen response element in the U3 region of the XMRV LTR.

REFERENCES

1. Urisman, A., et al., Identification of a novel Gammaretrovirus in prostate tumors of patients homozygous for R462Q RNASEL variant. PLoS Pathog, 2006. 2(3): p. e25.

2. Schlaberg R., Choe D. J., Brown K. R., Thaker H. M., and I. R. Singh (2009) XMRV is present in malignant prostatic epithelium and is associated with prostate cancer, especially high-grade tumors. Proc. Natl. Acad. Sci. USA, 106:16351-16356

3. Rodriguez J.J. and S.P. Goff, Xenotropic Murine Leukemia-Related Virus Establishes an Efficient Spreading Infection and Exhibits Enhanced Transcriptional Activity In LNCaP Prostate Cells. Manuscript submitted

XMRV is present in malignant prostatic epithelium and is associated with prostate cancer, especially high-grade tumors

Robert Schlaberg[a,1], Daniel J. Choe[b], Kristy R. Brown[a], Harshwardhan M. Thaker[b], and Ila R. Singh[a,b,2]

[a]Department of Pathology and Cell Biology, Columbia University Medical Center, 622 West 168th Street, New York, NY 10032; and [b]Department of Pathology, University of Utah, Emma Eccles Jones Medical Research Building, 15 North Medical Drive East, Salt Lake City, UT 84112

Communicated by Stephen P. Goff, Columbia University College of Physicians and Surgeons, New York, NY, July 20, 2009 (received for review April 29, 2009)

Xenotropic murine leukemia virus–related virus (XMRV) was recently discovered in human prostate cancers and is the first gammaretrovirus known to infect humans. While gammaretroviruses have well-characterized oncogenic effects in animals, they have not been shown to cause human cancers. We provide experimental evidence that XMRV is indeed a gammaretrovirus with protein composition and particle ultrastructure highly similar to Moloney murine leukemia virus (MoMLV), another gammaretrovirus. We analyzed 334 consecutive prostate resection specimens, using a quantitative PCR assay and immunohistochemistry (IHC) with an anti-XMRV specific antiserum. We found XMRV DNA in 6% and XMRV protein expression in 23% of prostate cancers. XMRV proteins were expressed primarily in malignant epithelial cells, suggesting that retroviral infection may be directly linked to tumorigenesis. XMRV infection was associated with prostate cancer, especially higher-grade cancers. We found XMRV infection to be independent of a common polymorphism in the *RNASEL* gene, unlike results previously reported. This finding increases the population at risk for XMRV infection from only those homozygous for the *RNASEL* variant to all individuals. Our observations provide evidence for an association of XMRV with malignant cells and with more aggressive tumors.

Gleason | immunohistochemistry | retrovirus | RNaseL | xenotropic

Prostate cancer is the most common form of nonskin cancer in U.S. men (1). The lifetime risk for developing prostate cancer is ≈1 in 6 (2) in the United States, and globally, 3% of men die of prostate cancer (3). Morbidity and mortality from prostate cancer are likely to grow further, given increasing longevity. Epidemiologic studies indicate that infection and inflammation may play a role in the development of prostate cancer (4, 5). A search for viral nucleic acids in prostate cancers led to the identification of xenotropic murine leukemia virus–related virus (XMRV) in ≈10% of samples tested (6). Because only malignant tissues were analyzed in the initial report, an association of XMRV with prostate cancer could not be addressed. Our analysis of 233 cases of prostate cancers and 101 benign controls showed an association of XMRV infection with prostate cancer, especially with more aggressive tumors. XMRV proteins were almost exclusively expressed in malignant epithelial cells. Only rarely did we find XMRV proteins in benign stromal cells, in contrast to a previous report (6).

XMRV was originally discovered in patients with a reduced activity variant of the *RNASEL* gene, and a strong correlation between this variant (R462Q) and the presence of XMRV was reported: 89% of XMRV-positive cases and only 16% of XMRV-negative cases were homozygous (QQ) for this variant in a total of 86 cases (6). Our study of 334 cases allowed us to establish the independence of XMRV infection and the R462Q variant. This finding moves the population at risk for XMRV infection from a small, genetically predisposed fraction homozygous for the R462Q *RNASEL* variant to all men. Sequence comparisons have classified XMRV as a gammaretrovirus with a high similarity to murine leukemia viruses. We present experimental evidence that XMRV is indeed a gammaretrovirus. Gammaretroviruses cause leukemias and sarcomas in multiple rodent, feline, and primate species but have not yet been shown to cause cancers in humans. Taken together, our findings provide evidence consistent with a direct oncogenic effect of this recently discovered retrovirus. If established, a direct role for XMRV in prostate cancer tumorigenesis would open up opportunities to develop new diagnostic markers as well as new methods to prevent and treat this cancer with antiretroviral therapies or vaccines.

Results

A Molecular Clone of XMRV Infects Human Prostate Cells. We constructed pXMRV1, a full-length XMRV molecular clone, using 2 overlapping clones from patient isolate VP62 (6) [gift of Don Ganem, University of California, San Francisco (UCSF)]. pXMRV1 was transfected into 293T cells. Reverse transcriptase (RT) activity was detected in the supernatant within 1–2 days of transfection (Fig. 1*A*), indicating the release of viral particles. These were inoculated onto naive 293T cells and LNCaP cells, a human prostate cancer cell line (American Type Culture Collection CRL-1740). Viral release from infected LNCaP cells was first seen on day 7 postinoculation and peaked at day 12. No particles were released from similarly inoculated 293T cells up to day 14. pXMRV1 is therefore an infectious molecular clone, and XMRV replicates efficiently in human prostate cells.

XMRV Particles Have Type-C Retrovirus Morphology. Particles released from XMRV-infected cells closely resembled those of a gammaretrovirus, Moloney murine leukemia virus (MoMLV), in size and morphology (Fig. 1 *B–E*). XMRV particles had an average diameter of 137 nm (SD = 9 nm), a spherical to somewhat pleomorphic shape, and characteristic lipid envelopes. The majority of particles contained an electron-dense, polygonal core with an irregular outline (average diameter 83 nm, SD = 8 nm), resembling mature type-C retroviral cores (Fig. 1*C*). Cores defined as "immature," i.e., spherical with an electron-lucent center, were also seen (Fig. 1*D*). A "railroad track," a term used to describe immature MoMLV cores (7), and formed by the radial alignment of the N- and C-terminal halves of the CA protein, was also seen in immature XMRV cores (Fig. 1*D*, arrowhead). These striking ultrastructural similarities between XMRV and MoMLV (Fig. 1*E*) suggest that the 2 viruses are assembled in a very similar manner.

XMRV Proteins, Except for Env, Closely Resemble Those of MoMLV. We identified XMRV proteins and defined their molecular weights by

Author contributions: H.M.T. and I.R.S. designed research; R.S., D.J.C., and K.R.B. performed research; R.S., H.M.T., and I.R.S. analyzed data; and R.S. and I.R.S. wrote the paper.

The authors declare no conflict of interest.

Freely available online through the PNAS open access option.

[1]Present address: Department of Pathology, University of Utah, Salt Lake City, UT 84112.

[2]To whom correspondence should be addressed. E-mail: ila.singh@path.utah.edu.

This article contains supporting information online at www.pnas.org/cgi/content/full/0906922106/DCSupplemental.

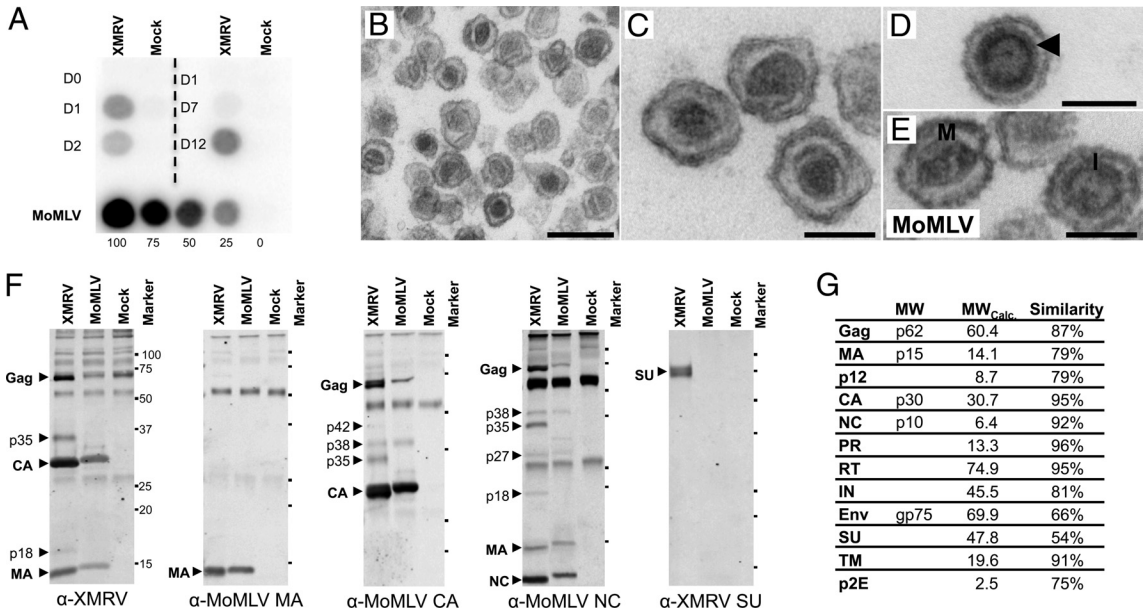

G

	MW	$MW_{Calc.}$	Similarity
Gag	p62	60.4	87%
MA	p15	14.1	79%
p12		8.7	79%
CA	p30	30.7	95%
NC	p10	6.4	92%
PR		13.3	96%
RT		74.9	95%
IN		45.5	81%
Env	gp75	69.9	66%
SU		47.8	54%
TM		19.6	91%
p2E		2.5	75%

Fig. 1. The XMRV molecular clone produces infectious particles with morphology and composition similar to MoMLV. (*A*) Viral release from cells transfected or inoculated with pXMRV1 or XMRV, respectively. (*Left*) Reverse transcriptase (RT) activity in culture supernatants from cells transfected with pXMRV1 or control EGFP plasmid. (*Right*) RT activity from LNCaP cells inoculated with XMRV. (*Lower*) RT activity from NIH 3T3 cells chronically infected with MoMLV shown for comparison. (*B–E*) Transmission electron microscopy of XMRV particles (*B*), mature XMRV cores (*C*), immature XMRV core, with ''railroad track'' marked by arrowhead (*D*), and MoMLV particles with mature (''M'') and immature (''I'') cores (*E*). (*F*) Western blot analysis of lysed XMRV and MoMLV virions, using antisera to XMRV whole virus, MoMLV-CA, MoMLV-MA, MoMLV-NC, and XMRV-Env SU. Comparison of blots allows identification of intermediates of Gag proteolysis, e.g., p27 (MA-p12), p42 (p12-CA), and p38 (CA-NC). (*G*) Molecular weights of XMRV proteins as calculated by Western blot analysis and by sequence prediction and similarity between XMRV and MoMLV proteins. [Scale bars: 250 nm (*B*) and 100 nm (*C–E*).]

comparing Western blots of lysed XMRV and MoMLV virions probed with antisera specific to XMRV or to MoMLV Gag proteins (Fig. 1 *F* and *G*). In accordance with their high (≈90%) sequence similarities, the molecular weights of XMRV and MoMLV Gag proteins were found to be very similar. We identified a 75-kDa band as the surface unit (SU) of the envelope (Env) protein, using rabbit antiserum specific to XMRV-Env SU. This antiserum did not react with the MoMLV-SU, consistent with the lower sequence similarity (54%) of the corresponding Env proteins and the general tendency of Env proteins to show greater evolutionary divergence, as compared to Gag or Pol proteins.

XMRV Proviral DNA Is Detected in 6% of Human Prostate Cancers; Viral Loads of XMRV Are Low. Our quantitative (q)PCR was designed to efficiently amplify XMRV proviral DNA from formalin-fixed, paraffin-embedded (FFPE) tissues. Primers and probes were chosen in a region of the integrase gene that is 100% conserved between all 3 published XMRV isolates and yet shares at most 80% similarity with the most closely related murine retroviral sequences (Fig. S1*A*). A common forward primer was used with 2 different reverse primers to allow for sequence differences in clinical isolates. Our qPCR was specific for XMRV sequences and did not amplify murine or human endogenous retroviruses; no amplification products were seen when using C57BL/6 mouse genomic DNA or human placental DNA as template. We tested the sensitivity of our qPCR assay in 2 ways. First, in the presence of excess human placental DNA, we could consistently detect 50 copies of the XMRV proviral clone and 5 copies 50% of the time (Fig. S1*B*). Second, because formalin fixation and embedding in paraffin compromise DNA quality, we also used fixed templates to test sensitivity. When DNA from FFPE human prostate tissue sections was spiked with known dilutions of DNA from fixed and embedded XMRV-infected, cultured cells, we consistently detected 1–2 infected cells per qPCR sample (Fig. S1*C*). We developed a second qPCR targeting the single-copy gene–vesicle-associated membrane protein 2 (VAMP2) to test for DNA integrity and amplification inhibitors [details in supporting information (*SI*) *Text*].

To estimate the prevalence of XMRV in men with and without prostate cancer, we analyzed 233 consecutively accessioned prostate cancers and 101 cases of transurethral resection of the prostate (TURP) as benign controls (Fig. S1*D*). We detected XMRV DNA in 14 (6.2%) cases of prostate cancer and in 2 (2.0%) controls. We determined XMRV proviral loads in these tissues. Using XMRV plasmid DNA as a standard, we estimated that qPCR-positive prostate cancers contained 1–10 copies of XMRV DNA per 660 diploid cells (see *Materials and Methods* and Fig. S1*E*). Because the number of tumor cells in any given section varies widely between tumors and even between different areas in the same tumor, it is impossible to estimate how many copies of XMRV DNA are present in each *tumor* cell. Using FFPE XMRV-infected cells as standards, we calculated that each 10-μm section from a prostate cancer contained the same amount of proviral DNA as 6–7 XMRV-infected cultured cells.

XMRV Protein Is Expressed in 23% of Prostate Cancers and Is Predominantly Seen in Malignant Epithelium. We developed XMRV-specific antisera and used them for immunohistochemistry (IHC). We first used XMRV-infected and uninfected cells that were mixed at different ratios and fixed in formalin and embedded in paraffin to mimic prostate tissue sections. We saw granular cytoplasmic staining in cells in proportion to the percentage of infected cells in the corresponding mixtures (Fig. 2 *A–C*). No staining was seen in uninfected cells or with preimmune serum (Fig. S2 *A* and *B*), confirming the specificity of our assay. We next performed IHC on prostate samples from XMRV qPCR-positive cases. We saw the same cytoplasmic granular pattern in tissues as in infected cultured cells (Fig. 2 *D* and *E*). Antiserum from a second rabbit resulted in identical staining. No staining was seen with preimmune serum (Fig. 2*F*).

We tested tissue sections from all 334 cases of prostate cancer and

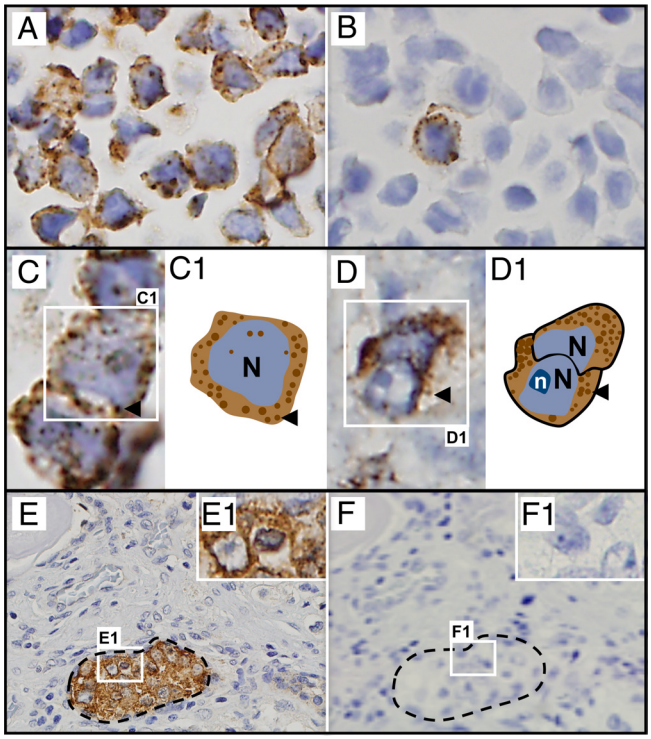

Fig. 2. XMRV proteins detected in infected cultured cells and in prostate cancer tissue by IHC, using anti-XMRV antiserum. Counterstaining with hematoxylin reveals blue nuclei. (*A* and *B*) XMRV-infected cells: 100% infected (*A*) and 1% infected (*B*). (*C*) Cultured infected cells at higher magnification show cytoplasmic granular staining, represented diagrammatically in *C1* (arrowhead, granules). (*D–F*) Human prostate cancers with clusters of malignant epithelial cells (*E*), with *Inset* at higher magnification (*E1*). Granular staining pattern seen at higher magnification. (*F* and *F1*) Adjacent section stained with preimmune serum from the same rabbit. N, nucleus; n, nucleolus.

controls with benign prostatic hyperplasia. We found XMRV protein expression in 54 (23%) cases with prostate cancer and in 4 (4%) controls (Fig. 4*A*). In contrast to a previous report (6) that found XMRV-specific staining only in nonmalignant stromal cells, we observed XMRV-specific staining predominantly in malignant prostatic epithelial cells. XMRV proteins were expressed in epithelial cells in 46 tumors (85%), in both epithelial and stromal cells in 4 tumors (7.5%), and exclusively in stromal cells in another 4 tumors (7.5%). Of the 4 controls, XMRV expression was seen in epithelial cells in 3 and in both epithelial and stromal cells in 1 case. Epithelial cells expressing XMRV protein usually belonged to a single acinus or to a few adjacent acini. The proportion of cells expressing XMRV protein in a given tissue section varied widely (Fig. 3 *A–G*) but positive cells always represented a minority of cells on the slide. The vast majority of IHC-positive epithelial cells showed the same granular staining pattern of the entire cytoplasm that was seen in cultured cells (Fig. 3 *A–F*). However, the staining intensity and the subcellular pattern varied between cases, ranging from intense staining of the entire cytoplasm (Fig. 3*E*) to more discrete granular staining (Fig. 3 *C* and *D*), with some unusual staining patterns (Fig. 3*G*). In summary, XMRV proteins were expressed in 23% of prostate cancers and 4% of controls. Protein expression was seen in clusters of malignant epithelial cells and very rarely in stromal cells (Fig. 3 *H* and *I*).

Presence of XMRV Correlates with Prostate Cancer and Higher Tumor Grade. We tested for a correlation of XMRV positivity (by qPCR or IHC) with the presence, grade, and stage of prostate cancer. XMRV positivity was 5-fold higher in cancer than in benign controls (odds ratio = 5.7, $P < 0.0001$, Fig. 4*A*). We also tested for a correlation between XMRV positivity and tumor grade as measured by the Gleason score. We saw a correlation between XMRV positivity and higher-grade cancers (Fig. 4*B*). Of the 233 cases with cancer, we found XMRV positivity in 18% of Gleason 6 tumors, 27% of Gleason 7 tumors, 29% of Gleason 8 tumors, and 44% of Gleason 9 tumors (χ^2-test for trend, $\chi^2 = 3.466$, $P = 0.06$, df = 1). Because only 1 case was a Gleason 10, it was not included in the analysis.

Most radical prostatectomy specimens contain relatively low pathological tumor–node–metastasis (TNM) stage cancers, because surgical treatment is not usually performed for higher stages. This is reflected in the distribution of tumor stages (pT) in our series: 75% pT2, 23% pT3, and 2% pT4. XMRV was detected in 25% of stage pT2 tumors and in 32% of pT3 tumors. Of the 5 cases with a pT4 stage, 1 (20%) was XMRV positive (Fig. 4*C*). This moderately increased prevalence of XMRV in advanced stage cancers was not statistically significant. Our sample had very few cases with nodal (N) metastasis and no cases with known distant metastases (M), preventing an investigation of a possible association of XMRV with higher N and M stages. We saw no association between XMRV infection and age at diagnosis (Fig. 4*D*).

XMRV Infection Is Independent of the R462Q Polymorphism of *RNASEL*. XMRV was initially discovered in prostate cancers from men homozygous for a common variant of the antiviral enzyme RNase L. This R462Q amino acid substitution results in a 3-fold reduction of enzymatic activity (8). In their study of 86 men with prostate cancer, Urisman et al. reported that 89% of XMRV-positive cases were homozygous for the R462Q variant (QQ) as compared to 16% of XMRV-negative cases (6). We profiled our 334 cases for the RNase L R462Q variant. The distribution was similar between cases with prostate cancer and controls (42.9% RR, 47.2% RQ, and 9.9% QQ in cancers vs. 52.5% RR, 40.6% RQ, and 6.9% QQ in controls, Fig. 4*E*). There was also no difference in allelic distribution between XMRV PCR-positive (50% RR, 43% RQ, and 7% QQ) and PCR-negative cases (42.7% RR, 47.4% RQ, and 10% QQ; Fig. 4*E*). The 2 XMRV-positive controls had RR alleles. When IHC was used to define XMRV-positive and -negative cases, the relative allelic distributions were also similar. We thus found no association between the presence of XMRV and the RNase L R462Q variant.

Discussion

XMRV is a candidate infectious agent for causing prostate cancer. On the basis of sequence comparison, XMRV was classified as a xenotropic murine gammaretrovirus. We present the first experimental evidence in support of this classification. The morphology of XMRV particles was very similar to MoMLV, a related murine gammaretrovirus. Protein products of the 2 viruses had similar molecular weights, and antisera to most proteins of each virus. The notable exception to this was the SU portion of Env, which determines host specificity and sets xenotropic viruses apart from other related murine viruses. XMRV SU-specific antisera did not cross-react with MoMLV-SU, and the 2 proteins share only a 54% similarity (as opposed to 75–96% similarity for other viral proteins). Our findings thus support the classification of XMRV as a xenotropic murine gammaretrovirus.

We developed 2 sensitive and specific assays for the detection of XMRV in tissues. We used these qPCR and IHC assays to demonstrate the presence of XMRV DNA or proteins in 27% of cases in the largest series of human prostate cancers analyzed thus far. We show that XMRV proteins are expressed almost exclusively in cancerous epithelial cells. Moreover, the presence of XMRV correlated with more aggressive, i.e., higher-grade tumors. These findings provide support for a possible oncogenic effect of XMRV and are crucial for designing studies to investigate mechanisms of transformation.

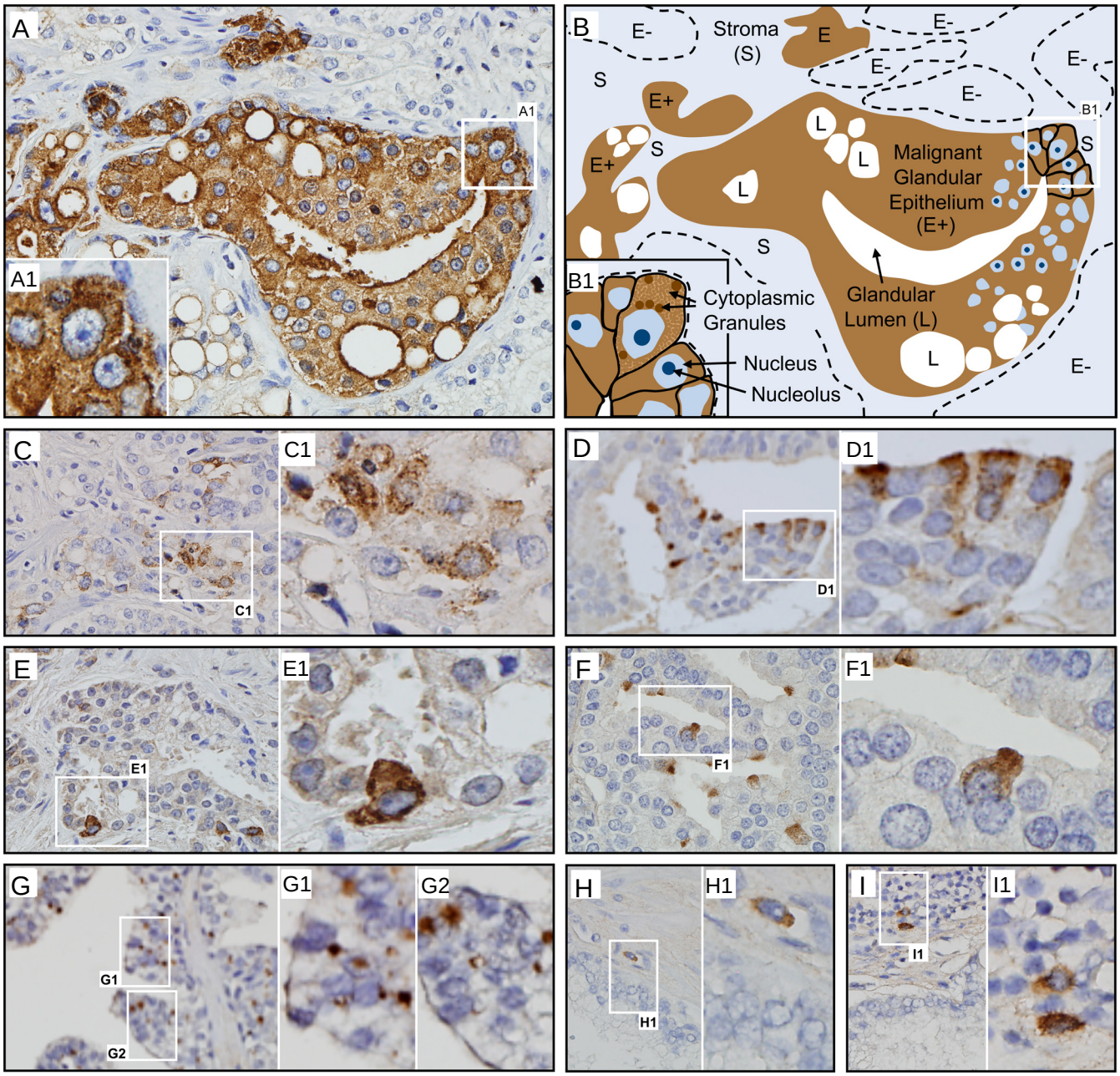

Fig. 3. XMRV proteins are expressed primarily in malignant epithelial cells and very rarely in stromal cells. (*A* and *B*) IHC of a section from a qPCR-positive prostate cancer (*A*) and its diagrammatic representation (*B*). Nuclei of malignant cells are large and contain ≥1 large nucleoli (*B*). Multiple acini of malignant epithelial cells (E+) stain positive. All cells within these acini show intense staining. The stroma (S) and a few other acini (E−) are unstained. *Insets* (*A1* and *B1*) show corresponding fields at higher magnification, with granular cytoplasmic staining pattern in several malignant epithelial cells. (*C*) A different field from the same sample as in *A* shows the range of XMRV protein expression in various acini: fewer cells expressing less protein but the same granular staining pattern. (*D–F*) Three additional representative samples with different frequencies of malignant epithelial cell clusters and different extents of XMRV protein expression. The intracellular staining pattern remains granular in all. (*G*) Staining limited to part of the cytoplasm of malignant epithelial cells in a subset of samples, as in this sample from which the XMRV clone VP62 was isolated, courtesy of R. H. Silverman and C. Magi-Galluzzi, Cleveland Clinic (6). (*H* and *I*) Scattered rare stromal cells showing cytoplasmic staining were seen close to malignant cells (*H*) or within inflammatory infiltrates (*I*).

The fraction of cases positive for XMRV by qPCR (6%) was lower than by IHC (23%). This variation can be attributed to sampling differences in conjunction with very low viral loads. For the qPCR, detection rates depend on the *proportion* of XMRV-infected cells in the tissue. DNA from infected cells gets diluted in DNA from uninfected cells, thus limiting sensitivity if only a few cells in the sample harbor XMRV. However, qPCR allows a rapid survey of large numbers of tissue samples. In contrast, IHC detects individual XMRV-infected cells, avoiding the dilution effect of PCR. However, the number of cells analyzed is much smaller by IHC (a 5-μm section vs. a 100-μm section for DNA extraction) and only actively replicating virus can be detected. Because XMRV produces focal, low-level infections, the 2 assays complement each other and using both is likely to lead to the most accurate estimate of prevalence.

Two of our findings differ significantly from the initial report on XMRV (6). First, we found XMRV proteins in malignant epithelial cells in contrast to initial reports of XMRV proteins in nonmalig-

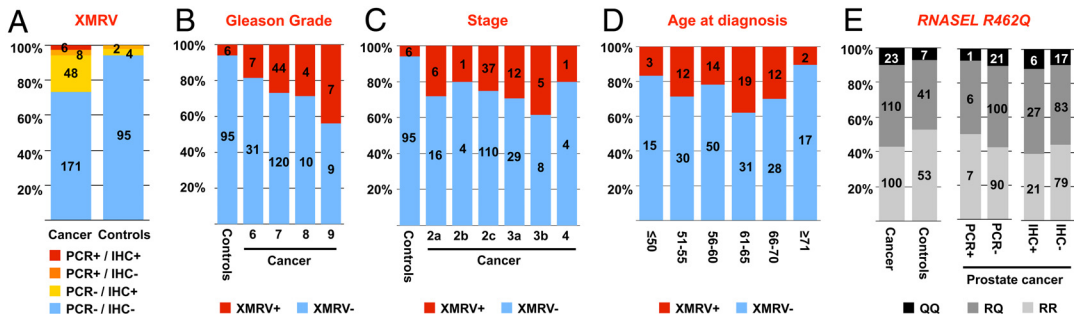

Fig. 4. XMRV DNA and proteins were more prevalent in prostate cancer than in controls, and especially frequent in high-grade cancers, and there was no correlation between presence of XMRV and any particular *RNASEL* genotype. (*A*) Number of prostate cancers or controls that were positive or negative for XMRV, either by qPCR or by IHC. (*B–D*) XMRV-positive cases (by either IHC or qPCR) correlated with Gleason grades (*B*), tumor stage (*C*), or age at diagnosis (*D*). (*E*) Presence of XMRV DNA or protein and the *RNASEL* genotype. Relative frequencies of RR, RQ, and QQ alleles in *RNASEL* at residue 462 were compared in prostate cancer cases and controls (*Left*), in cancers that tested positive or negative for XMRV DNA by qPCR (*Center*), and in cancers that tested positive or negative for XMRV proteins by IHC (*Right*). Cases are shown as percentages of total on the *y* axis and as number of cases within columns.

nant stromal cells. This can be mostly explained by our use of XMRV-specific antiserum instead of the monoclonal antibody to spleen focus-forming virus Gag protein used in the initial report. We were also able to detect XMRV in malignant epithelium from a case in the initial report (Fig. 3*G*), supporting the notion that antisera specific to XMRV offer a more sensitive means of viral detection. Second, we did not see any association of XMRV with the RNase L R462Q polymorphism as described initially. Methodological differences might account for this discrepancy. We tested prostate cancers for the presence of XMRV DNA and protein, whereas Urisman et al. used a nested RT-PCR to amplify viral RNA. It is conceivable that the reduced-activity variant of RNase L has a more significant effect on the levels of XMRV RNA, rather than on infection per se. Given low viral loads, the chance of detecting XMRV RNA may, therefore, be greater in homozygous individuals. Alternatively, the strength of association may depend on allelic frequencies and prevalence of XMRV. The distribution of RNase L R462Q alleles differed significantly between the 2 studies (23% QQ, 16% RQ, 61% RR in the study by Urisman et al. vs. 10% QQ, 43% RR, and 47% RQ in this study). Consistent with our findings, a survey in Northern European patients identified 2 individuals with XMRV; neither was homozygous for R462Q (9). The independence of XMRV infection from the RNase L R462Q variant indicates that all individuals may be at risk for XMRV infection, not just the ≈10% of the population that is homozygous for R462Q. Preventive and antiviral measures will thus benefit a much larger at risk population.

Our finding that XMRV is present in cancerous epithelial cells has important implications for pathogenesis. If XMRV plays a role in prostate cancer development, but infects only nonmalignant stromal cells in the tumor as previously reported, new mechanisms of retroviral oncogenesis would need to be invoked. This finding has discouraged investigation of a causal role of XMRV in prostate cancer thus far. While such a new mechanism is possible, our findings are immediately compatible with classical mechanisms of cell transformation by retroviruses. Retroviruses follow 3 distinct pathways when transforming cells. The first is transduction by an oncogene, where a cell-derived oncogene such as *src* in the viral genome causes rapid transformation. The second is via an essential retrovirus gene transactivating cellular growth-promoting genes, as in the case of the Tax protein of HTLV-I that induces T cell leukemia (10, 11), or the Env protein of Jaagsiekte sheep retrovirus that induces lung cancer in sheep (12). XMRV contains no recognizable oncogene, but we do not understand each XMRV protein enough to rule out any role it might play in transactivation. Finally, there is the insertional activation of a cellular oncogene, a mechanism followed by most leukemia-causing murine gammaretroviruses. Multiple rounds of viral infection are typically needed for the activating insertion to occur. Cells containing the activating insertion are selected over others, leading over time to a distinctly clonal population. While a small number of XMRV integration sites have been sequenced from human prostate cancers (13, 14), no evidence of clonality has emerged yet. Furthermore, the mechanism of insertional activation requires that each cancer cell contains a provirus or, at a minimum, the regulatory sequences from 1 LTR. We estimated that qPCR-positive prostate cancers contained 1–10 copies of XMRV DNA per 660 diploid cells. Because the number of malignant cells in any section varies widely between cases and even between different sections in the same prostate, it is impossible to estimate how many copies of XMRV DNA are present in each *cancer* cell. Our IHC data show that not all malignant cells express XMRV proteins, a finding with 2 possible explanations. It is possible that the malignant cells that lack XMRV protein expression were never infected by XMRV at all—a possibility that is incompatible with any known mechanism of insertional activation by murine gammaretroviruses. Alternatively, it is possible that some XMRV-infected cells lose large portions of their proviral DNA over time, as seen in tumors induced by avian leukosis virus (ALV). In these ALV-induced tumors, an absence of proviral sequences essential for production of viral RNA in most cells, coupled with the absence of viral RNA in tumors, indicates that expression of viral genes is not required for maintenance of the tumor phenotype (15). More studies are required to determine whether XMRV plays any causal role in prostate cancer or whether the presence of the virus in malignant prostatic epithelium is simply a function of its preferential replication in prostate cancer cells.

In line with a slow mechanism for oncogenesis, detection of XMRV in 6% of our controls might indicate that XMRV causes cancer only after a long induction period. Alternatively, these cases may have cancer in an unsampled area of the prostate: TURP removes periurethral tissue whereas cancer usually arises in the periphery of the prostate. It is also possible that XMRV infection does not always lead to cancer. Because our study protocol involves de-identified samples, follow-up of these XMRV-positive controls is not possible.

The finding that XMRV replicates efficiently in a cell line derived from human prostate cancer but not in other human cell lines suggests a viral tropism that warrants further investigation. Is the virus associated with cancers in tissues other than the prostate or in gynecologic malignancies? How is XMRV transmitted? These are all intriguing questions that deserve further exploration. There is growing evidence that current prostate cancer screening algorithms result in early detection of cancers but do not effectively reduce mortality (16, 17). Many cases of prostate cancer are unlikely to manifest themselves during the patient's lifetime. There is a clear need for better markers to detect cancers that pose a significant

health threat and to specifically target these for therapy. XMRV, because of its association with more aggressive cancers, might provide such a marker. Furthermore, there are often cases where a screening test is positive, but no tumor is detected on multiple biopsies, leaving the patient and his physician with no clear guidelines. A second XMRV-specific marker might provide further guidance. Large epidemiologic studies are needed to investigate correlation of XMRV with prostate cancer prognosis. The recognition that human papilloma viruses most often initiate cervical carcinomas has focused efforts on viral detection for early diagnosis and on preventive vaccination. Similarly, a determination that a retrovirus can cause prostate cancer would focus efforts on preventing transmission, antiviral therapy, and vaccine development. The pharmacological inhibition of viral replication, as achieved with HIV-1, could dramatically limit the pathological consequences of chronic viral infection.

Materials and Methods

Creating an Infectious Clone of XMRV. Overlapping partial clones AM-2–9 and AO-H4 derived from patient isolate VP62 (6) (gift of Don Ganem, UCSF) were used to generate pXMRV1, a full-length clone of XMRV with a CMV promoter (details of construction and sequencing are in *SI Text*).

Cell and Virus Production and Assay for Reverse Transcriptase Activity. 293T cells were maintained in DMEM and LNCaP cells in RPMI, both supplemented with 10% FBS, L-glutamine (2.2 mM), penicillin (100 units/mL), and streptomycin (100 μg/mL). Cells were transfected with plasmid pXMRV1 or control plasmid pEGFP-C1 (Clontech), using Lipofectamine PLUS (Invitrogen) following manufacturer's directions. Supernatants were harvested at regular intervals, passed through a 0.45-μm filter (Whatman), and monitored for virus production by measuring RT activity ((18), details in *SI Text*).

Transmission Electron Microscopy (TEM). Virions were centrifuged through 20% (wt/vol) sucrose, resuspended in 2.5% glutaraldehyde in 0.1 M Sorenson's buffer, and processed for TEM as described (19). Samples were analyzed on a JEOL JEM-1200 EXII electron microscope and photographed using an ORCA-HR digital camera (Hamamatsu). Diameters of 100 virions and cores were measured in Adobe Photoshop.

Anti-XMRV Antisera and Western Blot Analysis. For generation of XMRV whole virus antiserum (anti-XMRV), supernatant from cultured, infected cells was passed through a 0.22-μm filter (Pallcorp); centrifuged (18, 20); lysed with detergent and inoculated into rabbits (details in *SI Text*). The rabbits were bled before inoculation for preimmune control sera. Western blot analysis of concentrated virions was performed as previously described for MoMLV (18–20). XMRV proteins were visualized with primary rabbit anti-XMRV, anti-MoMLV CA (NCI 79S-804), anti-MoMLV MA (76S-155), anti-MoMLV NC (80S008, 1:7,500), and anti-XMRV-SU (1:500) antisera (MoMLV antisera and XMRV anti-XMRV-SU antisera were gifts of J. Rodriguez and S. P. Goff, Columbia University, New York). Data from at least 2 independent Western blots were used to determine XMRV protein sizes by comparison against molecular weight markers. MoMLV (NC_001501) was used for sequence comparisons.

Acquisition of Human Prostate Samples: Cancer and Control Tissues. Radical prostatectomy specimens (n = 233) acquired at the Columbia University Medical Center (CUMC) between August 2006 and December 2007 were used to estimate the prevalence of XMRV in human prostate cancer. Prostate tissues removed by TURP for benign prostatic hyperplasia between January 2007 and April 2008 were used as controls (n = 101). Details of tissue acquisition by banks, specimen selection, and processing are described in *SI Text*. Protected health information was removed and samples were de-identified by the tissue bank. Information about age at time of surgery, ethnicity, tumor stage, and tumor grade was retained (Table S1). Experiments were performed in accordance with the Institutional Review Board of CUMC (IRB-AAAC0089).

DNA Extraction from Human Prostate Tissues. DNA was extracted from 10 sections (10-μm thick) of FFPE tissue, quantified (Nanodrop 1000, Thermo Scientific), and stored at −80 °C (details in *SI Text*).

Quantitative PCR Amplification of Proviral DNA. BLAST analysis of overlapping 250-bp segments of the XMRV genome (VP35, GenBank ID DQ241301.1) identified a region of the integrase gene of XMRV that is 100% conserved between VP35, VP42, and VP62 but shares only 80–85% sequence identity with the most similar murine retroviruses. A forward primer, a hydrolysis probe, and 2 reverse primers were selected from this region using PrimerExpress (Applied Biosystems) (details in Table S2 and *SI Text*).

Immunohistochemistry. FFPE cultured XMRV-infected cells and prostate tissues were sectioned at 5-μm thickness and used for IHC. Details of sectioning, antigen retrieval, antibody treatment, counterstaining, protocol optimization, and controls are in *SI Text*.

RNase L Genotyping. The TaqMan SNP genotyping assay (assay ID: C___935391_1_), with the TaqMan SNP Genotyping Mix (both from Applied Biosystems), were used for RNase L G1385A (R462Q) genotyping (NCBI SNP reference: rs486907). Nine nanograms of prostatic DNA was used in a reaction volume of 20 μL. A TaqMan 7500Fast instrument was used for amplification, detection, and allelic discrimination. *RNASEL* genes from 2 individuals of each genotype were sequenced to confirm allelic discrimination results. DNA from 1 individual of each genotype was used as control in each subsequent experiment.

ACKNOWLEDGMENTS. We thank Drs. J. L. DeRisi and D. Ganem (UCSF) for clones AM-2–9 and AO-H4 and Drs. R. H. Silverman and C. Magi-Galluzzi (Cleveland Clinic) for prostate tissues from patients VP62 and VP45, and Drs. S. P. Goff and J. Rodriguez of Columbia University Medical Center (CUMC) for the XMRV-SU antisera. We thank Drs. H. Hibshoosh and B. Tycko (CUMC) for advice human tissue samples, the staff of the Histology and Immunohistochemistry Laboratories (Pathology Department) and the Tissue Bank (Herbert Irving Comprehensive Cancer Center, both at CUMC), especially S. Alexander, L. Yang, T. Wu, J. Cusmai, and K. Sun. We thank P. M. Pringle for queries of clinical databases, J. Smith for equipment maintenance (both at CUMC), and Drs. M. M. Mansukhani (CUMC) and V. Planelles (University of Utah) for generously sharing space and equipment. We thank Drs. S. P. Goff, V. Planelles, and D. R. Hillyard (University of Utah) for reading of the manuscript. This work was supported by grant PC060433 from the Department of Defense (to I.R.S.).

1. Jemal A, et al. (2008) Cancer statistics, 2008. *CA Cancer J Clin* 58(2):71–96.
2. Hayat MJ, Howlader N, Reichman ME, Edwards BK (2007) Cancer statistics, trends, and multiple primary cancer analyses from the Surveillance, Epidemiology, and End Results (SEER) Program. *Oncologist* 12(1):20–37.
3. Parkin DM, Bray FI, Devesa SS (2001) Cancer burden in the year 2000. The global picture. *Eur J Cancer* 37(Suppl 8):S4–S66.
4. De Marzo AM, et al. (2007) Inflammation in prostate carcinogenesis. *Nat Rev Cancer* 7(4):256–269.
5. Hayes RB, et al. (2000) Sexual behaviour, STDs and risks for prostate cancer. *Br J Cancer* 82(3):718–725.
6. Urisman A, et al. (2006) Identification of a novel Gammaretrovirus in prostate tumors of patients homozygous for R462Q RNASEL variant. *PLoS Pathog* 2(3):e25.
7. Yeager M, Wilson-Kubalek EM, Weiner SG, Brown PO, Rein A (1998) Supramolecular organization of immature and mature murine leukemia virus revealed by electron cryo-microscopy: Implications for retroviral assembly mechanisms. *Proc Natl Acad Sci USA* 95(13):7299–7304.
8. Casey G, et al. (2002) RNASEL Arg462Gln variant is implicated in up to 13% of prostate cancer cases. *Nat Genet* 32(4):581–583.
9. Fischer N, et al. (2008) Prevalence of human gammaretrovirus XMRV in sporadic prostate cancer. *J Clin Virol* 43(3):277–283.
10. Matsuoka M, Jeang KT (2007) Human T-cell leukaemia virus type 1 (HTLV-1) infectivity and cellular transformation. *Nat Rev Cancer* 7(4):270–280.
11. Grassmann R, Aboud M, Jeang KT (2005) Molecular mechanisms of cellular transformation by HTLV-1 Tax. *Oncogene* 24(39):5976–5985.
12. Cousens C, et al. (2007) In vivo tumorigenesis by Jaagsiekte sheep retrovirus (JSRV) requires Y590 in Env TM, but not full-length orfX open reading frame. *Virology* 367(2):413–421.
13. Dong B, et al. (2007) An infectious retrovirus susceptible to an IFN antiviral pathway from human prostate tumors. *Proc Natl Acad Sci USA* 104(5):1655–1660.
14. Kim S, et al. (2008) Integration site preference of xenotropic murine leukemia virus-related virus, a new human retrovirus associated with prostate cancer. *J Virol* 82(20):9964–9977.
15. Payne GS, et al. (1981) Analysis of avian leukosis virus DNA and RNA in bursal tumours: Viral gene expression is not required for maintenance of the tumor state. *Cell* 23(2):311–322.
16. Andriole GL, et al. (2009) Mortality results from a randomized prostate-cancer screening trial. *N Engl J Med* 360(13):1310–1319.
17. Schroder FH, et al. (2009) Screening and prostate-cancer mortality in a randomized European study. *N Engl J Med* 360(13):1320–1328.
18. Telesnitsky A, Blain S, Goff SP (1995) Assays for retroviral reverse transcriptase. *Methods Enzymol* 262:347–362.
19. Auerbach MR, Brown KR, Singh IR (2007) Mutational analysis of the N-terminal domain of Moloney murine leukemia virus capsid protein. *J Virol* 81(22):12337–12347.
20. Yuan B, Li X, Goff SP (1999) Mutations altering the moloney murine leukemia virus p12 Gag protein affect virion production and early events of the virus life cycle. *EMBO J* 18(17):4700–4710.

Supporting Information

Schlaberg et al. 10.1073/pnas.0906922106

SI Text

Creating an Infectious Clone of XMRV. Overlapping partial clones AM-2–9 and AO-H4 derived from patient isolate VP62 (1) and contained in pCR2.0-TOPO (Invitrogen) were a gift of Don Ganem, UCSF. Site-directed mutagenesis using complementary primers XMRV-M1 and XMRV-M2 (Table S2) was used to introduce a unique MluI restriction site into the overlapping segments of the 2 plasmids (QuikChange II site, Stratagene). The XMRV fragment from one plasmid was joined to the other at this MluI restriction site to obtain the full-length XMRV molecular clone pXMRV33 in pCR2.0-TOPO. The XMRV proviral sequence was then transferred to pcDNA3.1 using HindIII and NotI restriction sites in the pCR2.0-TOPO multiple cloning site (Invitrogen), to generate pXMRV1, a full-length clone of XMRV with a CMV promoter. pXMRV1 sequence was compared with that of the parent XMRV isolate VP62 (EF185282, Table S2). The 2 sequences differed at amino acid residue 411 of RT (M→V) because of substitutions introduced by the MluI restriction site (numbering according to MoMLV sequence NP_955591.1). Three additional differences (C→G at nucleotide 7450, 7694insT, and 7776insG) might represent sequence variations specific to VP62, or sequencing errors in VP62, because at each of these locations, the sequence of pXMRV1 is identical to that of 2 other sequenced clinical isolates of XMRV (2), VP35 (DQ241301.1) and VP42 (DQ241302.1).

Acquisition of Human Prostate Samples: Cancer and Control Tissues. Radical prostatectomy specimens (n = 233) submitted between August 2006 and December 2007 to the Department of Pathology and to the Tissue Bank of the Herbert Irving Comprehensive Cancer Center, Columbia University Medical Center were used to estimate the prevalence of XMRV in human prostate cancer. Prostate tissue specimens removed by transurethral resection for benign prostatic hyperplasia between January 2007 and April 2008 were used as controls. Controls known to contain incidental prostate cancer foci were not included in the study, leaving 101 controls. Of the 233 cancers, 95 were formalin-fixed, paraffin-embedded samples and 195 were frozen samples (with both specimen types available for 57 cases). Hematoxylin and eosin (H&E) stained sections from paraffin-embedded tissue blocks (ranging from 20 to 30 for each case) were examined for the presence of cancer. For each case, the block with the highest amount of cancer was chosen. Because prostate cancer foci cannot always be identified macroscopically at the time of frozen tissue sampling, an H&E-stained section of each case was examined by a pathologist for presence of cancer. Only 20% of our frozen tissue samples contained prostate cancer.

For controls, we collected 101 cases of prostatic tissue removed by transurethral resection of prostate (TURP), most commonly for benign prostatic hyperplasia. It is quite possible that some of these may have had cancer in a part of the prostate not removed by TURP, because prostate cancer usually arises in the periphery of the gland, whereas TURP mostly removes central tissue (Fig. S1*D*). If 1 TURP tissue block was available from a case, the one containing the highest amount of glandular tissue was chosen. The same tissue blocks were used for DNA extraction and immunohistochemical analysis.

DNA Extraction from Human Prostate Tissues. DNA was extracted from 10 sections (10-μm thick) of formalin-fixed, paraffin-embedded tissue, using the QIAamp DNA FFPE Tissue Kit (Qiagen) following manufacturer's directions. Microtome stages were cleaned with 10% bleach and 100% ethanol before each tissue block. New microtome blades were used for each case. The same method was used for extracting DNA from fresh frozen tissue, except the deparaffinization step was omitted. To reduce the risk of sample contamination, tissue processing, DNA extraction, and qPCR were performed in a separate laboratory.

Testing for DNA Integrity in Tissue Samples. We developed a qPCR targeting the single-copy gene–vesicle-associated membrane protein 2 (VAMP2) to test for DNA integrity and amplification inhibitors. Average amounts of amplifiable DNA were similar across sample types: mean quantification cycle (C_q) = 25 for frozen cancers (SD = 1.1), 26.4 for fixed cancers (SD = 3.4), and 25.6 for fixed controls (SD = 1.8). The DNA quality in XMRV PCR-positive cases was similar to that of XMRV PCR-negative cases as seen from equivalent C_q values in both groups. The average template quality was thus similar across sample types. Individual samples were considered unacceptable when the C_q for VAMP2 was 2 SD above the mean; thus, 5 (2.6%) frozen cancers, 7 (7.4%) fixed cancers, and 2 (2%) control samples were excluded from further qPCR analyses.

Quantitative PCR Amplification of Proviral DNA. The reaction mix for qPCR contained 1× TaqMan Fast Universal PCR Master Mix (Applied Biosystems), 900 nM forward and reverse primers, 250 nM hydrolysis probe, and 20–200 ng DNA in a reaction volume of 20 μL. As a positive control, 500 copies of pXMRV33 diluted in 200 ng human placental DNA (Sigma-Aldrich) were used. Thermocycling conditions were 95 °C for 20 sec, followed by 45 cycles of 95 °C for 3 sec and 60 °C for 30 sec, using MicroAmp Fast Optical 96-Well Reaction Plates and a TaqMan 7500Fast instrument (Applied Biosystems). All reactions were performed in duplicate. Serial 10-fold dilutions of plasmid pXRMV33 in 200 ng human placental DNA were used to validate the assay. To assess quality of DNA extracted from each tissue, a 168-bp segment of the single-copy gene VAMP2 (also known as Synaptobrevin 2) was amplified in a separate reaction. The reaction mix consisted of 1× TaqMan Fast Universal PCR Master Mix, 900 nM primers VAMP2–3043F and VAMP2–3210R, 250 nM hydrolysis probe VAMP2P, and 10–100 ng DNA in a total reaction volume of 20 μL. For positive control, 100 ng human placental DNA was used. Thermocycling conditions were the same as for detection of XMRV. For all primer sequences see Table S2.

Serial dilutions of the XMRV proviral clone were prepared in 200 ng of human placental DNA (50,000–5 copies/reaction). For formalin-fixed template standards, XMRV-infected cultured cells were serially diluted in uninfected cells at ratios of 1:100–1:1,000,000, fixed with formalin, and embedded in paraffin. One section of each dilution was added to 9 sections of normal prostate and DNA was extracted using the same method described above. To calculate the number of XMRV-infected cells contained in formalin-fixed qPCR standards, XMRV IHC-positive cells were counted in a section of infected cells diluted at a ratio of 1:100,000. For the remaining dilutions, the number of infected cells per section was extrapolated.

Immunohistochemistry. Formalin-fixed, paraffin-embedded prostate tissue sections were cut 5-μm thick, placed on electrostatically charged microscope slides, dried at 56 °C, deparaffinized in xylene, and rehydrated in decreasing alcohol concentrations.

Initial studies were performed with prostate sections from XMRV qPCR-positive cases. A strongly staining case was chosen for further optimization of the protocol. For antigen retrieval, sections were immersed in High pH Target Retrieval solution (Dako), pressure cooked (National SR-206-N) for 5 min, and slowly cooled to room temperature. Endogenous peroxidase activity was blocked with 3% H_2O_2. Sections were incubated with anti-XMRV antisera, diluted 1:7,500 in antibody diluent with background reducing components (Dako) in individual wells of Antibody Amplifier boxes (Prohisto). Tissue sections were incubated for 30 min with secondary anti-rabbit HRP-conjugated polymer antibody. Washes were with 50 mM Tris-HCl, 150 mM NaCl, 0.1% Tween-20, pH 8.0, and staining was detected with 3,3′-diaminobenzidinetrahydrochloride (Dako). Sections were counterstained with hematoxylin, dehydrated with graded alcohols, and covered with coverslips.

1. Urisman A, et al. (2006) Identification of a novel Gammaretrovirus in prostate tumors of patients homozygous for R462Q RNASEL variant. *PLoS Pathog* 2(3):e25.
2. Jemal A, et al. (2008) Cancer statistics, 2008. *CA Cancer J Clin* 58(2):71–96.

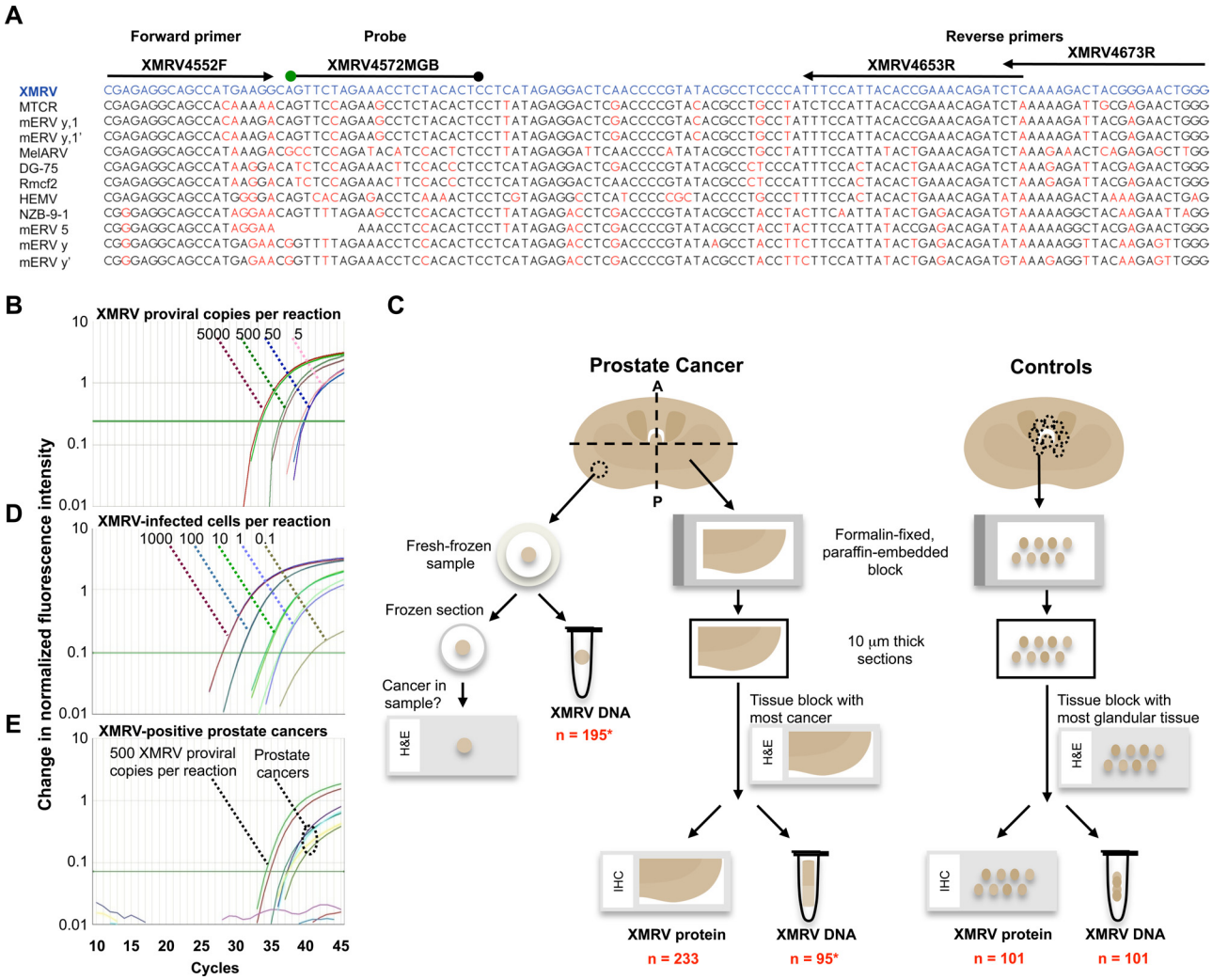

Fig. S1. Detection of XMRV DNA in prostate tissues by a qPCR and scheme for processing tissues for DNA extraction and immunohistochemistry. (*A*) Primer and probe hybridization sites in the XMRV integrase gene compared with equivalent regions of the most closely related murine retroviral sequences. For abbreviations and accession numbers, see Table S2. (*B* and *C*) Sensitivity of the qPCR assay: Detection of 5-5,000 copies of XMRV molecular clone in 200 ng human placental DNA (*B*). Serial 10-fold dilutions containing DNA from FFPE cultured XMRV-infected cells. No amplification was seen with uninfected cells (*C*). With both methods, the lowest detectable template concentrations resulted in quantification cycles (C_q) between 36 and 40. (*D*) Analysis of 233 consecutive cases of prostate cancer resections and 101 controls. Cancers consisted of frozen (n = 138), FFPE (n = 38), or frozen and fixed (n = 57) tissues. All controls were FFPE tissues. A, anterior; P, posterior; H&E, hematoxylin & eosin staining; *, for 57 cases, both frozen and fixed tissues were tested. (*E*) C_q for XMRV-positive prostate cancer samples compared to that for a standard reaction containing 500 copies of XMRV proviral DNA diluted in normal prostatic DNA.

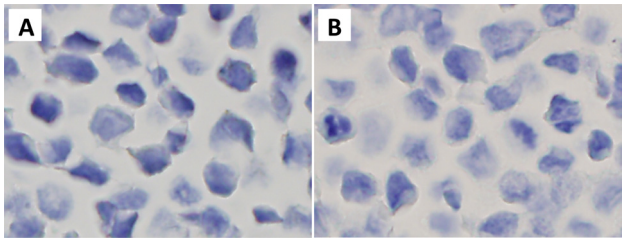

Fig. S2. Specificity of detection of XMRV proteins by IHC. (*A*) Using anti-XMRV antiserum on mock-infected cells results in no staining. (*B*) Similarly, no staining is observed when pre-immune serum from the same rabbit is used to stain XMRV-infected cells. Counterstaining with hematoxylin reveals blue nuclei.

Table S1. Samples acquisition with demographic information, tumor grade, and stage

	Prostate cancer				
Sample type	All	Frozen	Fixed	Both	Controls: fixed
Number	233	138	38	57	101
Age, median (range)	60 (41–76)	60 (41–74)	60 (43–76)	61 (50–73)	72 (44–85)
Race/ethnicity, %					
African–American	17	19	16	14	27
Caucasian	53	55	53	49	38
Hispanic	12	13	8	14	29
Other/not provided	17	13	24	23	6
Tumor grade, %					NA
6	16.3	18.1	10.5	15.8	
7	70.4	71.0	73.7	66.7	
8	6.0	4.3	10.5	7.0	
9	6.9	5.8	5.3	10.5	
10	0.4	0.7	0	0	
Tumor stage, %					
Primary tumor					NA
pT2a	9	13	5	4	
pT2b	2	2	3	2	
pT2c	63	57	79	67	
pT3a	18	19	11	19	
pT3b	6	7	3	4	
pT4	2	1	0	5	
Regional LN					NA
pNX	54	52	58	54	
pN0	44	46	40	42	
pN1	2	1	3	4	

Age is given in years and tumor grade is given as the Gleason score. Tumor stage is according to the American Joint Committee on Cancer (1): pT2a, unilateral, involving one-half of 1 lobe or less; pT2b, unilateral, involving more than one-half of 1 lobe but not both lobes; pT2c, bilateral disease; pT3a, extraprostatic extension; pT3b, seminal vesicle invasion; pT4, invasion of bladder, rectum; pNX, regional lymph nodes were not assessed; pN0, no regional lymph node metastasis; pN1, metastasis in regional lymph node(s). Distant metastasis was not assessed in any of the patients with prostate cancer. Abbreviations: LN, Lymph node; NA, not applicable.

1. Jemal A, et al. (2008) Cancer statistics, 2008. *CA Cancer J Clin* 58(2):71–96.

Table S2. Sequences of primers used for mutagenesis, sequencing, and qPCR

Primer	Start position	Sequence	Application
XMRV-M1	3,800	5′-CCT TGC CTA CGc gTG GTA GCA GCC-3′	Mutagenesis
XMRV-M2	3,823	5′-GGC TGC TAC CAc gCG TAG GCA AGG-3′	Mutagenesis
XMRV-S1R	602	5′-CGA GAA CAC TTA AAG ACA GAA GAA-3′	Sequencing
XMRV-S2R	944	5′-CGG GAG CTG TCG GTA A-3′	Sequencing
XMRV-S1F	1,339	5′-TGA AGA TCC AGG TAA ATT GAC G-3′	Sequencing
XMRV-S3R	1,575	5′-TCT GTA GTG GTG TAA TCC CAA TC-3′	Sequencing
XMRV-S2F	3,733	5′-GGG ACC TTG GCG TCG GCC TGT GGC-3′	Sequencing
XMRV-S4R	3,853	5′-CTT GCC TGC ATC CTT TGT CA-3′	Sequencing
XMRV-S3F	5,522	5′-GCC GCT GCT TAT CAG GAC CAG-3′	Sequencing
XMRV-S5R	5,702	5′-GTA TCC ACG CAG AGA TGC C-3′	Sequencing
XMRV-S6R	5,731	5′-AGT TGT CGC CGC CTT TAC GTG-3′	Sequencing
XMRV-S4F	6,598	5′-GGG ACG GGA GAC AGG CT-3′	Sequencing
XMRV-S7R	6,761	5′-GGG GCA GAG GTA TGG TTG G-3′	Sequencing
XMRV-S5F	7,380	5′-TGG CGT AGT AAG AGA TAG CAT-3′	Sequencing
XMRV-S8R	7,567	5′-GAA TAC AGG GTC CGA AGA G-3′	Sequencing
XMRV-S6F	7,727	5′-ACC CCA CCA TAA GGC TTA GCA C-3′	Sequencing
XMRV-S9R	7,942	5′-TTA GTT TCG CTT TAT CTG AGG ACC A-3′	Sequencing
XMRV4552F	4,552	5′-CGA GAG GCA GCC ATG AAG G-3′	Detection
XMRV4572MGB	4,572	5′-6FAM AGT TCT AGA AAC CTC TAC ACT C MGBNFQ-3′	Detection
XMRV4653R	4,653	5′-GAG ATC TGT TTC GGT GTA ATG GAA A-3′	Detection
XMRV4673R	4,673	5′-CCC AGT TCC CGT AGT CTT TTG AG-3′	Detection
VAMP2–3043F	3,043	5′-TCT GCC ACT TCG GGT TTC TC-3′	Control
VAMP2–3210R	3,210	5′-GGT AGC CAC CCC TCT CAC AA-3′	Control
VAMP2P	3,067	5′-HEX CAT TCC TGC TCC CCA GTT TTC ATG TGG Tamra-3′	Control

MGBNFQ, minor grove binder/nonfluorescent quencher. Nucleotide positions are based on VP62 (EF185282.1).

Table S3. Sequences used for alignment and design of specific primers

Abbreviation	Definition (GenBank accession no.)
XMRV	XMRV VP35 (DQ241301.1)
	XMRV VP42 (DQ241302.1)
	XMRV VP62 (EF185282.1)
MTCR	Retroviridae complete genome, murine type C retrovirus (X94150.1)
	Mus musculus chromosome 1, clone RP24–65D16 (AC115959.17)
mERV y,1	*M. musculus* BAC clone RP24–320A8 from chromosome y (AC182253.3)
	M. musculus strain C57BL/6J chromosome 1 clone rp23–116m12 (AC083892.19)
mERV y,1′	*M. musculus* BAC clone RP24–320A8 from chromosome y (AC182253.3)
	M. musculus strain C57BL/6J chromosome 1 clone rp23–116m12 (AC083892.19)
MelARV	*M. musculus* isolate MelARV endogenous B-tropic ecotropic murine leukemia virus (DQ366148.1)
	M. musculus C-type ecotropic endogenous retrovirus (U63133.1)
DG-75	DG-75 Murine leukemia virus (AF221065.1)
	Murine AIDS virus-related provirus (S80082.1)
	M. musculus chromosome 9, clone RP23–364M24 (AC103610.9)
	M. musculus BAC clone RP23–277L21 from chromosome 2 (AC124194.3)
	Mouse DNA sequence from clone RP23–130L13 on chromosome 9 (CT009721.14)
	Mouse DNA sequence from clone RP23–259C9 on chromosome 13 (CT030655.7)
	Mouse DNA sequence from clone RP24–114E18 on chromosome 2 (AL928935.14);
	Mouse DNA sequence from clone RP23–354H24 on chromosome 4(AL627314.6)
	Mouse DNA sequence from clone RP23–384D6 on chromosome 4 (AL627077.14)
Rmcf2	*M. musculus castaneus* endogenous virus Rmcf2 (AY999005.1)
HEMV	Murine leukemia virus serotype HEMV provirus (AY818896.1)
NZB-9–1	Xenotropic murine leukemia virus isolate NZB-9–1 (EU035300.1)
mERV 5	*M. musculus* chromosome 5, clone RP23–110C17 (AC117614.14)
mERV y	*M. musculus* BAC clone RP24–163J18 from chromosome y (AC175744.2)
mERV y′	*M. musculus* BAC clone CH36–265C6 from chromosome y (AC202413.4)
	M. musculus BAC clone RP24–302I24 from chromosome Y (AC1 (1844409.3)

mERV, murine endogenous retrovirus.

Xenotropic Murine Leukemia-Related Virus Establishes an Efficient Spreading Infection and Exhibits Enhanced Transcriptional Activity In LNCaP Prostate Cells

XMRV Replication in Prostate cells

Jason J. Rodriguez[1] and Stephen P. Goff[1*]

Columbia University

Howard Hughes Medical Institute

HHSC 1313

701 W 168th St.

New York, NY 10032

Keywords: XMRV/Steroid/LTR/

*Corresponding author: tel: 212-305-3794, fax: 212-305-5106, spg1@columbia.edu

Abstract

Xenotropic Murine-Related Leukemia Virus (XMRV) is a novel human gamma retrovirus discovered in association with human prostate tumors. XMRV was first identified in prostate stromal cells surrounding the tumors of patients carrying a mutation in the *HPC1* gene locus. To determine the tropism of XMRV in cell culture, we tested the ability of XMRV to spread and replicate in various prostate and non-prostate cell lines. We found that while expression of XMRV viral proteins and spread of infectious virus were minimal in a variety of cell lines, XMRV displayed robust expression and infection in LNCaP prostate tumor cells. The transcriptional activity of the XMRV Long Terminal Repeat (LTR) was found to be higher than the Moloney Murine Leukemia virus (MoMLV) LTR in both LNCaP and WPMY-1 cells. The U3 promoter of XMRV and a glucocorticoid response element (GRE) within the U3 were required for the transcriptional activity in LNCaP cells. Co-expression of the androgen receptor (AR) and stimulation with dihydrotestosterone (DHT) stimulated XMRV-LTR dependent transcription in 293T cells and the GRE was required for this activity. These data suggest that XMRV may replicate more efficiently in LNCaP cells in part due to the transcriptional environment in LNCaP cells.

Introduction

Nearly 35% of familial prostate cancer patients carry a germ-line mutation (R462Q) in the HPC1 gene locus (1). This locus encodes the protein RNase L, which is expressed and activated upon virus infection and degrades single-stranded viral and cellular RNA, thus blocking replication of the infecting virus and inducing apoptosis (2,3). The association of prostate cancers with this variant of RNase L raised the possibility that mutant individuals were more susceptible to an unknown tumor virus (1,4). Total polyadenylated RNA from prostate tumors that were either heterozygous or homozygous for the mutant RNase L allele was isolated and hybridized to a DNA microarray (Virochip) containing oligomers of ~ 950 viral genomes (5). Seven of eleven tumors that carried at least one allele of the RNase L mutation were positive for the novel retrovirus. Isolation and sequencing of the virus from three different prostate cancer patients revealed nucleotide similarities to xenotropic MLVs, and the virus was named Xenotropic MLV-Related Virus (XMRV) (5). The genome structure of XMRV is typical of gamma retroviruses. The *Env* gene encodes a glycoprotein homologous to the MLV envelope protein that mediates virus binding to the xenotropic receptor, XPR1, on the surface of cells (6). In contrast to more complex retroviruses such as lentiviruses, XMRV does not encode any accessory genes, nor does it encode any host-derived oncogenes (7). Fluorescence in situ hybridization and immunohistochemistry revealed that a small number of stromal cells surrounding the tumor, but not tumor cells themselves, were positive for XMRV nucleotide sequences and viral proteins, suggesting that XMRV maintains a low level of infection in these tumors, and that direct oncogenesis by XMRV might not play a role in prostate tumorigenesis (5).

Recent studies have demonstrated the affinity of XMRV to prostate cells. XMRV was produced at high titers from approximately 10 integrated copies within the prostate carcinoma cell line 22Rv1 (8). Another study has confirmed the presence of XMRV infected cells within the prostate but differs significantly from the original report describing XMRV. XMRV was found in 23% of all prostate cancers without correlation to the RNaseL R462Q mutant allele. Significantly, malignant prostate epithelial cells were infected with XMRV at higher rate compared to stromal cells, thus leaving open the possibility of direct oncogenesis by XMRV (9). Amyloidogenic fragments known as semen-derived enhancer of virus infection (SEVI) from prostatic acid phosphatase increased XMRV infectivity at the level of virus entry. XMRV nucleic acid was also found in prostatic secretions of prostate cancer patients, suggesting a possible mechanism of transmission (10).

XMRV has been shown to be sensitive to the antiviral actions of interferon (IFN) (6), a well characterized antiviral mechanism against pathogenic infections (11). The DU145 prostate cell line treated with IFNβ prior to XMRV infection was more resistant to a spreading infection than cells without IFN (6). LNCaP prostate cells were permissive for XMRV infection in the presence or absence of IFN and were four times more supportive of virus infection than DU145 cells. The role that RNase L plays in regulating XMRV is still unclear: DU145 cells with a modest siRNA knockdown of RNase L showed slower rather than enhanced replication of XMRV, and there was no change in replication with or without IFN treatment (6). Moreover, it is also unknown what effect the R429Q mutation in RNase L plays in the general response against viral infection. The 3-fold decrease in catalytic activity associated with this mutation may not profoundly change the susceptibility of the cells (4).

Many simple retroviruses initiate tumors by insertional activation of proto-oncogenes: the viral promoter or enhancer elements cause elevated expression of one or more critical genes that lead to oncogenesis (reviewed in (12)). Other retroviruses can directly initiate oncogenesis via the activity of particular viral genes, with a prominent example being the *Env* protein from Jaagsiekte Sheep Retrovirus (JSRV) (13). Whether XMRV integrates into DNA elements that might contribute to prostate cancer formation was addressed by sequencing sites of proviral integration (6,14). XMRV followed a pattern most similar to MLV and integrated at sites near transcription start sites, CpG islands, and DNase-hypersensitive sites, consistent with the notion that XMRV integrates in areas of open chromatin (14). However, specific integration near proto-oncogenes in tumors or direct transformation by XMRV *in-vitro* has not been observed.

In this study, we determined the ability of infectious XMRV to replicate in cell lines derived from various tissues. Of the cell lines tested, XMRV replicated most efficiently in the LNCaP cell line of prostate origin. To explore why these prostate cells are more permissive for XMRV replication, we analyzed the transcriptional activity of the XMRV LTR in permissive and non-permissive cell lines. Consistent with the tropism of XMRV replication, an increased transcriptional activity was seen in LNCaP and WPMY-1 prostate cell lines. The U3 region of XMRV and a GRE was specifically required for this activity. The data presented in this study suggest that LNCaP prostate cells provide a transcriptional environment that supports efficient replication and spread of XMRV.

Materials and Methods

Cell Culture and Virus All cell lines were maintained at 37°C and 5% CO_2 and supplemented with 10% fetal bovine serum (Invitrogen). LNCaP cells (human prostate epithelial tumor cells, gift of the Gelmann lab) were maintained in RPMI 1640 (Invitrogen); PC-3 (human prostate epithelial tumor cells, ATCC) cells were maintained in Eagle's modified essential medium (Invitrogen); DU145 (human prostate epithelial cells, ATCC) were maintained in FK12 media (Invitrogen); 2fTGH (gift of Horvath lab, human fibrosarcoma), HeLa (ATCC, cervical carcinoma), TE671 (human rhabdomyosarcoma), Rat2 (rat fibroblast), and 293T (human embryonic kidney) cells were maintained in DMEM (Invitrogen). XMRV virus particles were generated by transfecting LNCaP cells with 5 µg of proviral DNAs. For XMRV spreading infection assays, LNCaP cell culture media was harvested eight days post infection and passed through a 0.45 µM filter and stored at -80°C. Polybrene (8 µg/ml) was added during virus harvesting. The relative concentration of XMRV in supernatants was determined by measuring the RT activity in cell culture media of harvested stocks (15).

Plasmids and Reagents The full length genome of XMRV (patient VP62) was obtained from Dr. Ganem (University of California, San Francisco). XMRV halves AM 2-9 and AO H4 (5) were joined by introducing a novel MluI site and performing overlapping PCR, which generated one amino acid change; glycine to alanine at position 385 of RT . The genome was ligated into pCR2-TOPO cloning vector. To generate the provirus, the U3 region was amplified and ligated to 5' R region. This proviral construct was also ligated into the pCR2-TOPO cloning vector and utilized for all subsequent experiments. pcDNA3.1(+) was utilized as a control

plasmid for generating mock virus stocks and as a control for mock provirus transfection. MoMLV and XMRV LTR (U3-R-U5-Gag start site) DNAs were amplified by PCR and cloned in between *NdeI* and *HindIII* sites by SLIC cloning into the plasmid pRL-null. The LTR fused to the start site of renilla luciferase was used as a reporter gene. The XM1 reporter plasmid in which the MoMLV U3 was swapped for the XMRV U3, was generated by SLIC cloning in the same manner as the full length LTRs. The mutant reporter, mGRE, was generated in the same fashion with the nucleotides 192 and 193 (adenine) of the full length LTR both being changed to cytosine. The androgen receptor (AR) expression and DHT was a gift from Liang-Nian Song of the Gelmann lab (Columbia University, (16)).

Preparation of Cell Lysates and Immunoblotting Transfected cells were lysed with NP40 lysis buffer (150 mM NaCl, 0.5% NP40, 50 mM Tris, pH 8.0, 0.5 mM EDTA) supplemented with protease inhibitor cocktail (Roche) at 4°C for 30 minutes. Equal amounts of protein from clarified extracts were added to protein loading buffer, boiled for 5 minutes, and subjected to SDS-PAGE. Proteins were transferred to nitrocellulose and immunoblotted with antisera against MoMLV CA (cross-reacts with XMRV Gag and CA) or GFP (Abcam; ab290-50).

XMRV Spreading Assays $1x10^5$ Cells were seeded onto 6-well dishes and infected the day after with 100 µl of LNCaP culture supernatants containing XMRV viral particles. The cells were allowed to recover after 8 hours of adsorption at 37°C with appropriate cell media. Samples were taken each day and subjected to reverse transcriptase assays described in (15) to

monitor release of viral particles into the culture supernatants. XMRV was isolated by ultracentrifugation of filter-sterilized (0.45 μm) supernatants at 25,000 rpm, 4°C for 2 hours. Virus pellets were lysed in NP40 lysis buffer supplemented with protease inhibitors and protein loading buffer. Samples were boiled, subjected to SDS-PAGE and immunoblotted using antisera against the MoMLV CA protein.

Luciferase Reporter Gene Assays

Luciferase reporter gene assays were performed according to manufacturer's protocol (Promega). 293T, LNCaP, or WPMY-1 cells were transfected with different reporter genes and lysed with passive lysis buffer 24 hours post transfection (hpt). For treatment with DHT, cells were exposed to 10 μM of DHT at the time of transfection. Luciferase activity was measured from triplicate samples using a POLARstar Omega plate reader (BMG labtech). All conditions represent the average values from triplicate samples, normalized to co-transfected firefly-luciferase (pcDNA4.0-Fluc).

Results

To generate infectious virus particles, we obtained the XMRV full length genome isolated from patient designated VP62 (5). The provirus was transfected into both 293T or LNCaP prostate cells and lysates of transfected cells were tested for XMRV Gag and CA accumulation two days post transfection (Figure 1). Both 293T and LNCaP lysates contained nearly the same amount of steady–state Gag and CA proteins. The transfection efficiency of LNCaP cells is extremely

poor, as indicated by the levels exogenously expressed GFP. Normalization of Gag proteins to co-transfected GFP levels suggests that LNCaP cells express a higher amount of Gag compared to 293T cells (Figure 1B).

To determine whether the XMRV particles are infectious, LNCaP culture media containing XMRV virus particles were applied to 293T or LNCaP cells (Figure 2A) and these infected cultures were monitored for virus release into the media by analyzing CA accumulation in the supernatants. At four and eight days post infection, distinctly higher levels of CA at steady-state were found in the culture media from infected LNCaP cells compared to 293T cells, suggesting that XMRV spreads more efficiently in LNCaP cells. Virion spread and release into the media was also examined by measuring the activity of reverse transcriptase in the cell culture supernatants (Figure 2B). LNCaP cells were supportive of an XMRV spreading infection, with peak RT activity detected at day three, and then continued at day seven, after the cells were re-seeded. RT activity in 293T cell culture supernatants, however, was not detected, indicating a lack of replication. Though 293T cells were poor producers of XMRV virus particles, we tested if the virions from 293T culture media were infectious by applying supernatants to naïve LNCaP or 293T cells and monitoring RT activity. While 293T cells did not support efficient XMRV replication and spread, LNCaP cells rescued the few virus particles produced from 293T cells and could then initiate a spreading XMRV infection (Figure 2C).

To further assess the cell line tropism of XMRV, we infected seven different cell lines with XMRV harvested from LNCaP cell culture supernatants. XMRV infection was conducted on LNCaP, 293T, HeLa (human cervical carcinoma), 2fTGH (human fibrosarcoma), TE671 (human rhabdomyosarcoma), and Rat2 (rat fibroblast) cells, and subsequent CA release into the culture media was examined (Figure 3A). Three days post-infection, CA could be detected in

the media supernatants from all cell lines, but LNCaP supernatants contained the highest levels. After six days, high levels of CA were observed in culture supernatants from LNCaP cells but not from the other cell lines, indicating that XMRV infection and spread was most efficient in LNCaP prostate cells. Next, we tested XMRV replication in three other prostate cell lines: DU145 prostate carcinoma cells, WPMY-1 prostate stromal cells, and PC-3 prostate carcinoma cells. As before, XMRV supernatants were applied to naïve cells and release of CA in the culture media was measured (Figure 3B). Compared to other prostate cell lines, LNCaP cells again were the most permissive for XMRV replication and spread, as monitored by CA production. RT release into the media was detected in LNCaP, DU145, and WPMY-1 cells (Figure 3C), with LNCaP cells supporting the most robust spreading infection.

These data indicate that XMRV preferentially replicates in the LNCaP human prostate cell line. The intracellular accumulation of XMRV Gag and CA to higher levels in LNCaP cells suggested the possibility that the promoter of XMRV displayed an enhanced level of transcription in these cells. We generated luciferase reporters that were fused to the LTRs of both MoMLV and XMRV, in which the fusion point was the translation initiation site of Gag (Figure 4A). We then tested the transcriptional output of these reporter genes by transfecting LNCaP, WPMY-1, or 293T cells with these DNAs and measuring luciferase activity (Figure 4B). The transcriptional activity of the MoMLV LTR was higher than the HSV-1 TK promoter in all cell lines tested, but the pattern of XMRV LTR activity in different cells was distinct. The XMRV LTR transcriptional activity was lower than that of MoMLV in 293T cells but higher in both LNCaP and WPMY-1 prostate cells.

Most, if not all, of the transcriptional activity of the retroviral LTR typically originates from cis-acting DNA elements within the U3 region that recruit various cellular transcription

factors. Whether the XMRV U3 was responsible for the enhancement of XMRV transcription in LNCaP and WPMY-1 cells was tested by generating a chimeric luciferase reporter gene in which the MoMLV U3 was replaced with the U3 of XMRV (Figure 4A) and tested for its transcriptional activity (Figure 4C). The chimeric reporter gene (XM1) behaved exactly like the full length XMRV LTR: transcriptional activity was lower than MoMLV LTR in 293T cells but higher in LNCaP and WMPY-1 prostate cells. Together, these data indicate that the U3 region of the XMRV LTR promotes transcription more efficiently in LNCaP and WMPY-1 prostate cell lines.

Xenotropic MLVs contain a glucocorticoid response element (GRE) within their U3 region which is conserved within the XMRV LTR. To determine whether the XMRV GRE binding site plays a role in transcription, the GRE was mutated (GAACAGATGG – G**CC**CAGATGG, mGRE) and the promoter activity of the mutant LTR (mGRE) was determined by luciferase assays (Figure 5). As seen before, transfection of 293T cells with the MoMLV LTR resulted in a higher luciferase activity than the XMRV LTR-driven reporter gene. The mutant mGRE reporter exhibited a minimal decrease in activity in 293T cells (Figure 5A). Significantly, the mutant mGRE reporter showed a four-fold reduction in LNCaP cells, suggesting that this DNA element may play a role in transcription from XMRV LTR (figure 5B). We next tested whether the androgen receptor (AR) can activate the XMRV-LTR reporter gene in 293T cells (Figure 5C). Co-expression of AR had no effect on the transcriptional activity of the XMRV LTR; however, following co-expression of AR and stimulation with dihydrotestosterone (DHT), an AR agonist, the activity increased to that of the MoMLV LTR. Importantly, mutation of the GRE site abolished activity with or without DHT stimulation and

AR co-expression. Co-expression with glucocorticoid receptor (GR) and treatment with dexamethasone, a GR agonist, had no effect on the XMRV reporter gene (data not shown).

Discussion

This study examines the tropism of XMRV in different culture cell lines. We found that expression of Gag and CA from the provirus of XMRV is more efficient in LNCaP cells compared to 293T cells. Similarly, LNCaP cells supported XMRV viral spread but 293T cells did not. The few virus particles that did arise from 293T cells could be rescued by transfer to LNCaP cells; thus, virions from 293T cells were not grossly defective. Of the prostate and non-prostate cell lines tested, LNCaP cells are the most efficient host cell line for spread of infectious XMRV. We analyzed the transcriptional output from the XMRV LTR and found that the U3 region provides a higher transcriptional activity than the constitutively highly active MoMLV LTR in LNCaP and WPMY-1 cells, but lower activity than the MoMLV LTR in 293T cells. These data suggest that the U3 promoter region of the XMRV LTR plays a significant role in transcriptional activity in LNCaP cells.

The U3 regions of xenotropic MLVs are conserved and contained transcriptional elements that regulate transcription of the integrated provirus (17,18). Transcription factors such as NF-1, E-box proteins, and C/EBP coordinate with other factors to activate transcription signals to RNA Polymerase II. Interestingly, the mouse xenotropic MLVs contain two GREs that are conserved within XMRV. Cells that constitutively express the AR, such as hormone-responsive prostate cells and LNCaP cells, are thus predicted to be susceptible to AR-dependent agonists and could stimulate transcription of XMRV. In support of this notion, co-expression of

the AR along with the XMRV LTR reporter in 293T cells and stimulation with DHT increased transcription. Mutation of one of the conserved GRE sequences abolished the transcriptional activity observed with DHT stimulation, suggesting AR and steroid responses do indeed play a role in XMRV replication. The hypothesis of whether AR expression and steroid exposure increases XMRV replication in its natural setting remain to be completed.

Alternative explanations for the enhanced replication of XMRV in LNCaP cells also exist. It is possible, for example, that the cellular receptor for XMRV, XPR1, may be expressed at a higher level in LNCaP cells than other cell types tested in this study. However, quantitative PCR analysis revealed that 293T cells express four-fold higher levels of XPR1 mRNA transcripts than LNCaP cells (supplemental Figure 1) suggesting that XPR1 does not account for the weak spreading infection of XMRV in 293T cells. We also considered the possibility that the lack of RNase L expression in LNCaP cells may be responsible for the permissiveness. To address the possibility, we depleted RNase L using RNA interference (RNAi) in 293T cells (supplemental Figure 2). Despite greater than 95% reduction in RNase L protein levels, XMRV replication was not enhanced (data not shown). However, it is possible that production of IFN may limit the spread of XMRV. Increasing amounts of IFN exposure in an IFN signaling-competent cell line reduced XMRV replication in a dose-dependent manner (6). LNCaP cells are known to be deficient in JAK1, and have impaired IFN signaling which may account for the robust spreading in this cell line (19). Experiments in which IFN antiviral signaling is restored in LNCaP cells will ultimately resolve this possibility.

This study shows that XMRV is capable of replicating efficiently in LNCaP prostate cells and induces the release of high levels of virus. This may in part be due to an enhanced transcriptional environment within LNCaP cells that allows for production of more viral proteins

and subsequent budding of viral particles. The increase in transcriptional activity of the XMRV LTR is totally attributable localized to the U3 region and requires a GRE sequence element within the U3. The data presented further indicate that XMRV transcription can be enhanced by steroids, suggesting that XMRV may show selectivity for hormone responsive cell types including the prostate.

Acknowledgements

This work was supported by PHS grant R37 CA 30488 from the National Cancer Institute. JJR was supported by an institutional training grant T32 CA 009503-21A1 from the NCI.

We thank the Horvath laboratory for their generosity with cells and reagents. We would also like to thank Drs. Hogg and Wolf for editorial advice. JJR is an Associate, and SPG is an Investigator of the Howard Hughes Medical Institute.

Figure Legends

Figure 1: LNCaP cells express a higher level of Gag and CA compared to 293T cells. (A) Cells were transfected with XMRV DNAs and a plasmid expressing exogenous GFP. Cell lysates were prepared 2 days post transfection (hpt) and characterized for expression of Gag, CA, and GFP levels by SDS-PAGE. (B) Normalization of Gag protein levels to co-expressed exogenous GFP. This experiment was performed in triplicate and the data shown is representative of one experiment.

Figure 2: XMRV spreads efficiently in LNCaP cells but not 293T cells. (A) Eight day culture media from LNCaP cells that were transfected with the XMRV provirus were adsorbed onto either naïve 293T or LNCaP cells. Virus spreading was monitored over eight days by immunoblotting supernatants against XMRV CA. XMRV 1:10: culture media was diluted ten-fold at time of infection. (B) Same as in A but monitoring RT activity over seven days. On the third day the cells were diluted and re-seeded to allow accumulation of XMRV virus particles. (C) Same as in A but culture media from 293T cells that were transfected with the XMRV provirus were adsorbed onto either naïve 293T or LNCaP cells.

Figure 3: XMRV spreading in LNCaP cells. (A) Same as in Figure 2, but different cell lines were infected with XMRV and levels of CA were measured by immunoblotting at three and six days post infection. 293T: human embryonic kidney cells, HeLa: human cervical carcinoma, 2fTGH: human fibrosarcoma, TE671: human rhabdomyosarcoma, Rat2: rat fibroblast. (B) Same as in A, but three prostate cell lines were tested: WPMY-1 (prostate stromal), DU145 (prostate

epithelial), and PC-3 (prostate epithelial). (C) RT assay measuring XRMV spread in three different prostate cell lines: LNCaP, DU145, and WPMY-1 cells.

Figure 4: XMRV LTR exhibits a higher transcriptional activity in LNCaP and WPMY-1 prostate cells. (A) Schematic diagram of MoMLV and XMRV LTR luciferase reporter gene constructs. The 5' LTR of both MoMLV and XMRV were fused to renilla luciferase at the translational start site for Gag. XM1: chimeric reporter gene where the U3 region of MoMLV was swapped for the U3 of XMRV (B) Reporter genes in A were transfected into 293T, LNCaP, or WPMY-1 cells and luciferase activity was measured 24 hours later. Null: luciferase with no promoter, TK: HSV-1 thymidine kinase promoter upstream of renilla luciferase. All samples were in triplicate and were normalized to co-transfected firefly luciferase. Data are represented as fold difference compared to Null control (Null = 1). (C) Same as in B but the XM1 reporter gene was included demonstrating the XMRV U3 is required for the observed transcriptional specificity in LNCaP and WMPY-1 cells.

Figure 5: The GRE site within the XMRV LTR is required for transcriptional activity. (A) 293T cells were transfected with the LTR reporter genes depicted in figure 4A and with a XMRV LTR containing a mutant within the GRE site (mGRE; GAACAGATGG – G**CC**CAGATGG). Luciferase activity was measured 24 hours later and normalized to co-transfected firefly luciferase. (B) Same as in A, but LNCaP cells were transfected. (C) Same as in A, but the XMRV LTR was co-transfected with the AR and treated with DHT for 24 hours post lysis. mGRE was included to demonstrate the mutation does not respond to AR expression

and DHT stimulation.

References

1. **Silverman, R.H.** 2003. Implications for RNase L in prostate cancer biology. Biochemistry **42**:1805-12.

2. **Bisbal, C. and T. Salehzada**. 2008. [RNase L, a crucial mediator of innate immunity and other cell functions]. Med Sci (Paris) **24**:859-64.

3. **Silverman, R.H.** 2007. Viral encounters with 2',5'-oligoadenylate synthetase and RNase L during the interferon antiviral response. J Virol **81**:12720-9.

4. **Casey, G., P.J. Neville, S.J. Plummer, Y. Xiang, L.M. Krumroy, E.A. Klein, W.J. Catalona, N. Nupponen, J.D. Carpten, J.M. Trent, R.H. Silverman, and J.S. Witte**. 2002. RNASEL Arg462Gln variant is implicated in up to 13% of prostate cancer cases. Nat Genet **32**:581-3.

5. **Urisman, A., R.J. Molinaro, N. Fischer, S.J. Plummer, G. Casey, E.A. Klein, K. Malathi, C. Magi-Galluzzi, R.R. Tubbs, D. Ganem, R.H. Silverman, and J.L. DeRisi**. 2006. Identification of a novel Gammaretrovirus in prostate tumors of patients homozygous for R462Q RNASEL variant. PLoS Pathog **2**:e25

6. **Dong, B., S. Kim, S. Hong, J. Das Gupta, K. Malathi, E.A. Klein, D. Ganem, J.L. Derisi, S.A. Chow, and R.H. Silverman**. 2007. An infectious retrovirus susceptible to an IFN antiviral pathway from human prostate tumors. Proc Natl Acad Sci U S A **104**:1655-60.

7. **Cullen, B.R.** 1992. Mechanism of action of regulatory proteins encoded by complex

retroviruses. Microbiol Rev **56**:375-94.

8. **Knouf, E.C., M.J. Metzger, P.S. Mitchell, J.D. Arroyo, J.R. Chevillet, M. Tewari, and A.D. Miller**. 2009. Multiple integrated copies and high-level production of the human retrovirus XMRV (xenotropic murine leukemia virus-related virus) from 22Rv1 prostate carcinoma cells. J Virol **83**:7353-6.

9. **Schlaberg, R., D.J. Choe, K.R. Brown, H.B. Thaker, and I.R. Singh**. 2009. XMRV is present in malignant prostatic epithelium and is associated with prostate cancer, especially high grade tumors. Proc. Nat. Acc. Sci. **106**:

10. **Hong, S., E.A. Klein, J. Das Gupta, K. Hanke, C.J. Weight, C. Nguyen, C. Gaughan, K.A. Kim, N. Bannert, F. Kirchhoff, J. Munch, and R.H. Silverman**. 2009. Fibrils of prostatic acid phosphatase fragments boost infections with XMRV (xenotropic murine leukemia virus-related virus), a human retrovirus associated with prostate cancer. J Virol **83**:6995-7003.

11. **Samuel, C.E.** 1994. Interferon-induced proteins and their mechanisms of action. Hokkaido Igaku Zasshi **69**:1339-47.

12. **Maeda, N., H. Fan, and Y. Yoshikai**. 2008. Oncogenesis by retroviruses: old and new paradigms. Rev Med Virol **18**:387-405.

13. **Palmarini, M. and H. Fan**. 2003. Molecular biology of jaagsiekte sheep retrovirus. Curr Top Microbiol Immunol **275**:81-115.

14. **Kim, S., N. Kim, B. Dong, D. Boren, S.A. Lee, J. Das Gupta, C. Gaughan, E.A. Klein,**

C. Lee, R.H. Silverman, and S.A. Chow. 2008. Integration site preference of xenotropic murine leukemia virus-related virus, a new human retrovirus associated with prostate cancer. J Virol **82**:9964-77.

15. **Goff, S., P. Traktman, and D. Baltimore**. 1981. Isolation and properties of Moloney murine leukemia virus mutants: use of a rapid assay for release of virion reverse transcriptase. J Virol **38**:239-48.

16. **Song, L.N., M. Coghlan, and E.P. Gelmann**. 2004. Antiandrogen effects of mifepristone on coactivator and corepressor interactions with the androgen receptor. Mol Endocrinol **18**:70-85.

17. **Verdin, E. and C. Van Lint**. 1995. Internal transcriptional regulatory elements in HIV-1 and other retroviruses. Cell Mol Biol (Noisy-le-grand) **41**:365-9.

18. **Tomonaga, K. and J.M. Coffin**. 1999. Structures of endogenous nonecotropic murine leukemia virus (MLV) long terminal repeats in wild mice: implication for evolution of MLVs. J Virol **73**:4327-40.

19. **Dunn, G.P., K.C. Sheehan, L.J. Old, and R.D. Schreiber**. 2005. IFN unresponsiveness in LNCaP cells due to the lack of JAK1 gene expression. Cancer Res **65**:3447-53.

Supplemental Figure 1: Analysis of XPR1 mRNA transcripts in various cell lines. Total mRNA isolated from LNCaP, WPMY-1, PC-3, HeLa, DU145, 293T, and 2fTGH cells were reverse transcribed to obtain cDNA. Triplicate RT products were amplified using primers for XPR1 or GAPDH by qPCR and SYBR Green reaction mix. Standard curves for both XPR1 and GAPDH were created and XPR1 values were normalized to GAPDH transcript levels. Data is represented as a fold difference against LNCaP XPR1 mRNA levels where LNCaP XPR1 = 1.

Supplemental Figure 2: Knockdown of RNase L in 293T cells. Lentivirsues harboring mir30shRNA (OpenBiosystems – pGIPZ) knockdown against RNase L or a scrambled control were produced and used to infect naïve 293T cells. Cells containing integrated RNAi were selected for by puromycin treatment and RNase L levels were measured by SDS-PAGE and immunoblotting against RNase L (Abcam, 2E9L). RNase L 53 and 56 are to distinct shRNA targeting constructs.

Figure 1

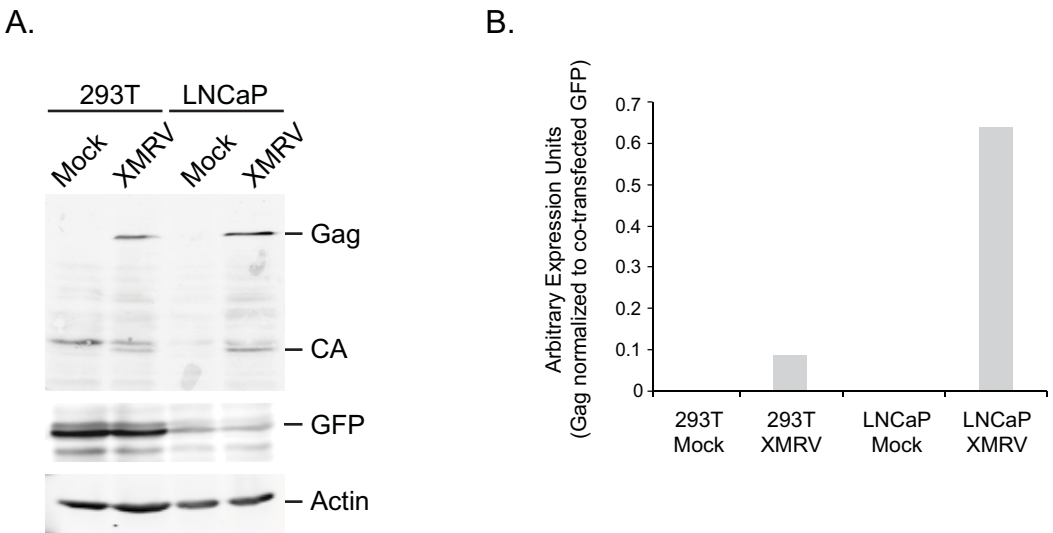
A.
293T
LNCaP
Mock
XMRV
Mock
XMRV
Gag
CA
GFP
Actin
B.
Arbitrary Expression Units
(Gag normalized to co-transfected GFP)
0.7
0.6
0.5
0.4
0.3
0.2
0.1
0
293T
Mock
293T
XMRV
LNCaP
Mock
LNCaP
XMRV

Figure 2

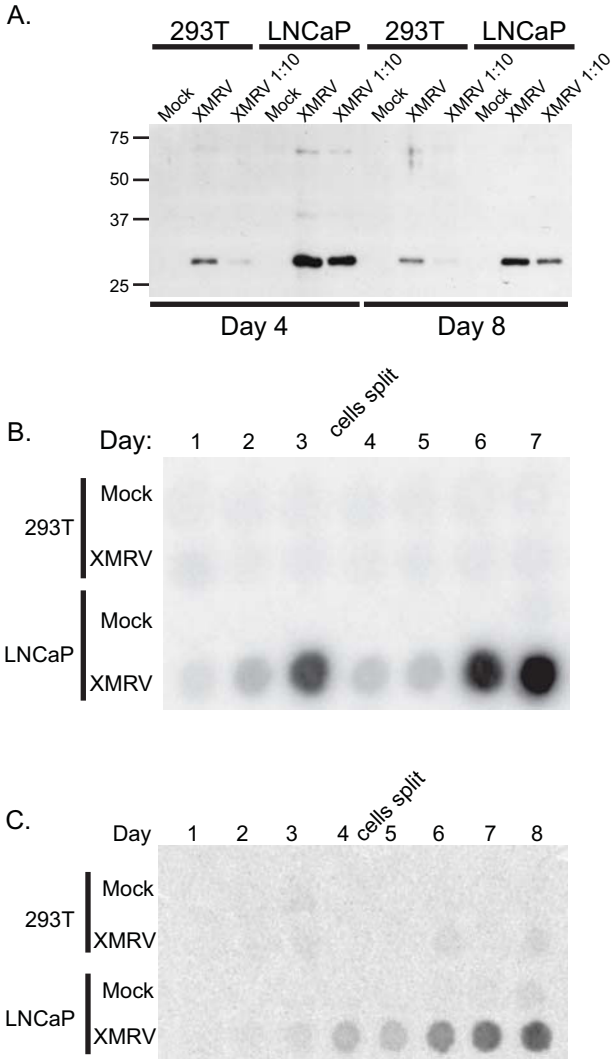
A.
293T
LNCaP
293T
LNCaP
Mock
XMRV
XMRV 1:10
Mock
XMRV
XMRV 1:10
Mock
XMRV
XMRV 1:10
Mock
XMRV
XMRV 1:10
75
50
37
25
Day 4
Day 8
B.
Day:
1
2
3
cells split
4
5
6
7
293T
Mock
XMRV
LNCaP
Mock
XMRV
C.
Day
1
2
3
4
cells split
5
6
7
8
293T
Mock
XMRV
LNCaP
Mock
XMRV

Figure 3

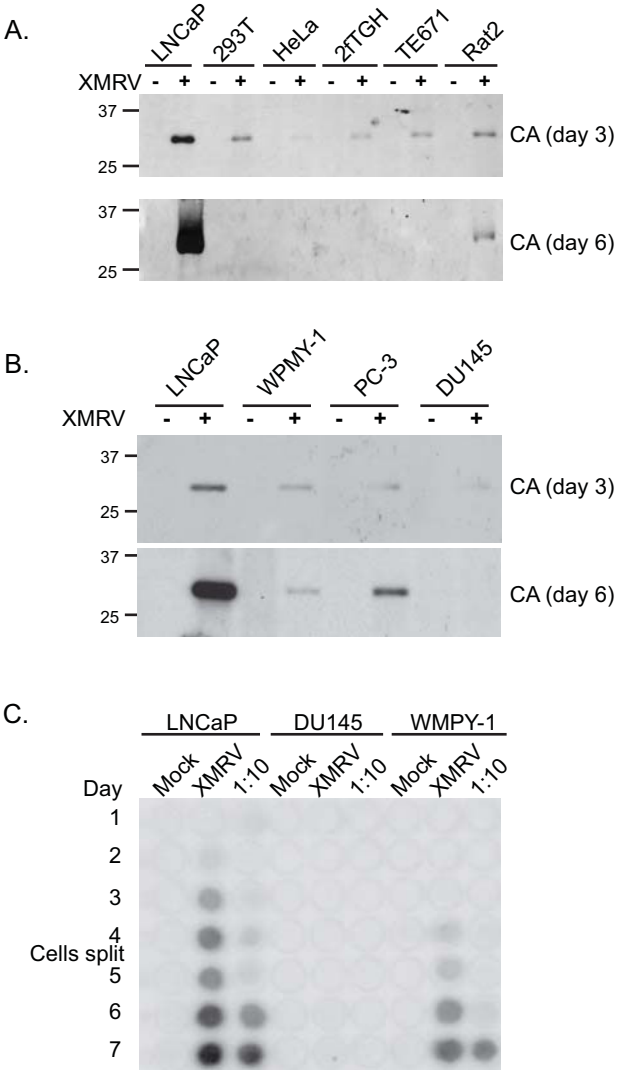
A.
LNCaP
293T
HeLa
2fTGH
TE671
Rat2
XMRV - + - + - + - + - + - +
37
25
CA (day 3)
37
25
CA (day 6)
B.
LNCaP
WPMY-1
PC-3
DU145
XMRV - + - + - + - +
37
25
CA (day 3)
37
25
CA (day 6)
C.
LNCaP
DU145
WMPY-1
Mock
XMRV
1:10
Day
1
2
3
4
Cells split
5
6
7

Figure 4

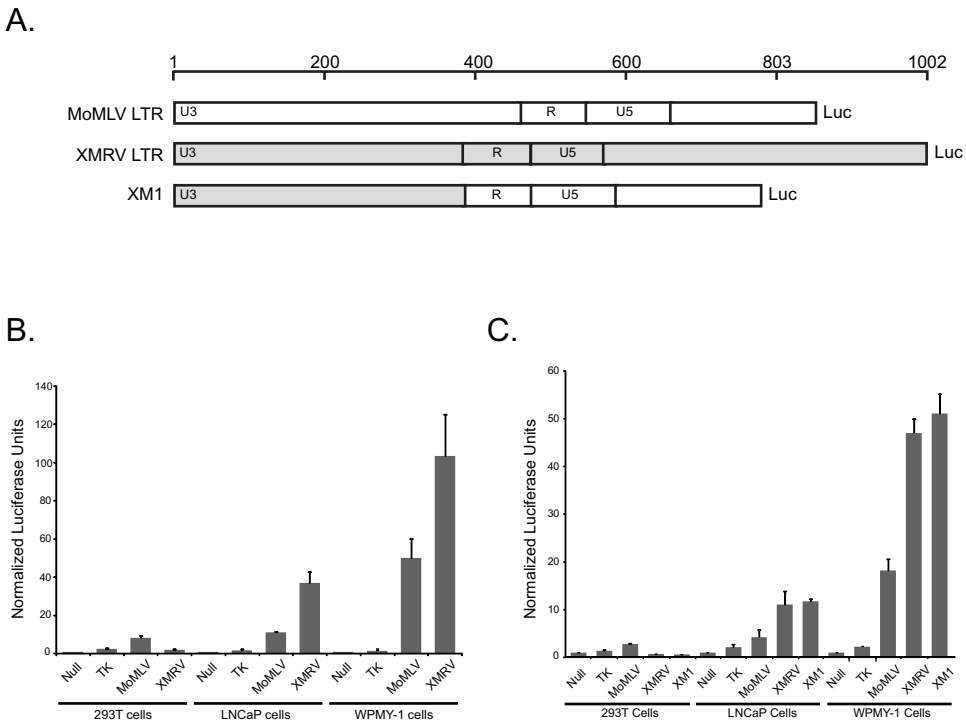
A.
1
200
400
600
803
1002
MoMLV LTR
U3
R
U5
Luc
XMRV LTR
U3
R
U5
Luc
XM1
U3
R
U5
Luc
B.
Normalized Luciferase Units
140
120
100
80
60
40
20
0
Null
TK
MoMLV
XMRV
Null
TK
MoMLV
XMRV
Null
TK
MoMLV
XMRV
293T cells
LNCaP cells
WPMY-1 cells
C.
Normalized Luciferase Units
60
50
40
30
20
10
0
Null
TK
MoMLV
XMRV
XM1
Null
TK
MoMLV
XMRV
XM1
Null
TK
MoMLV
XMRV
XM1
293T Cells
LNCaP Cells
WPMY-1 Cells

Figure 5

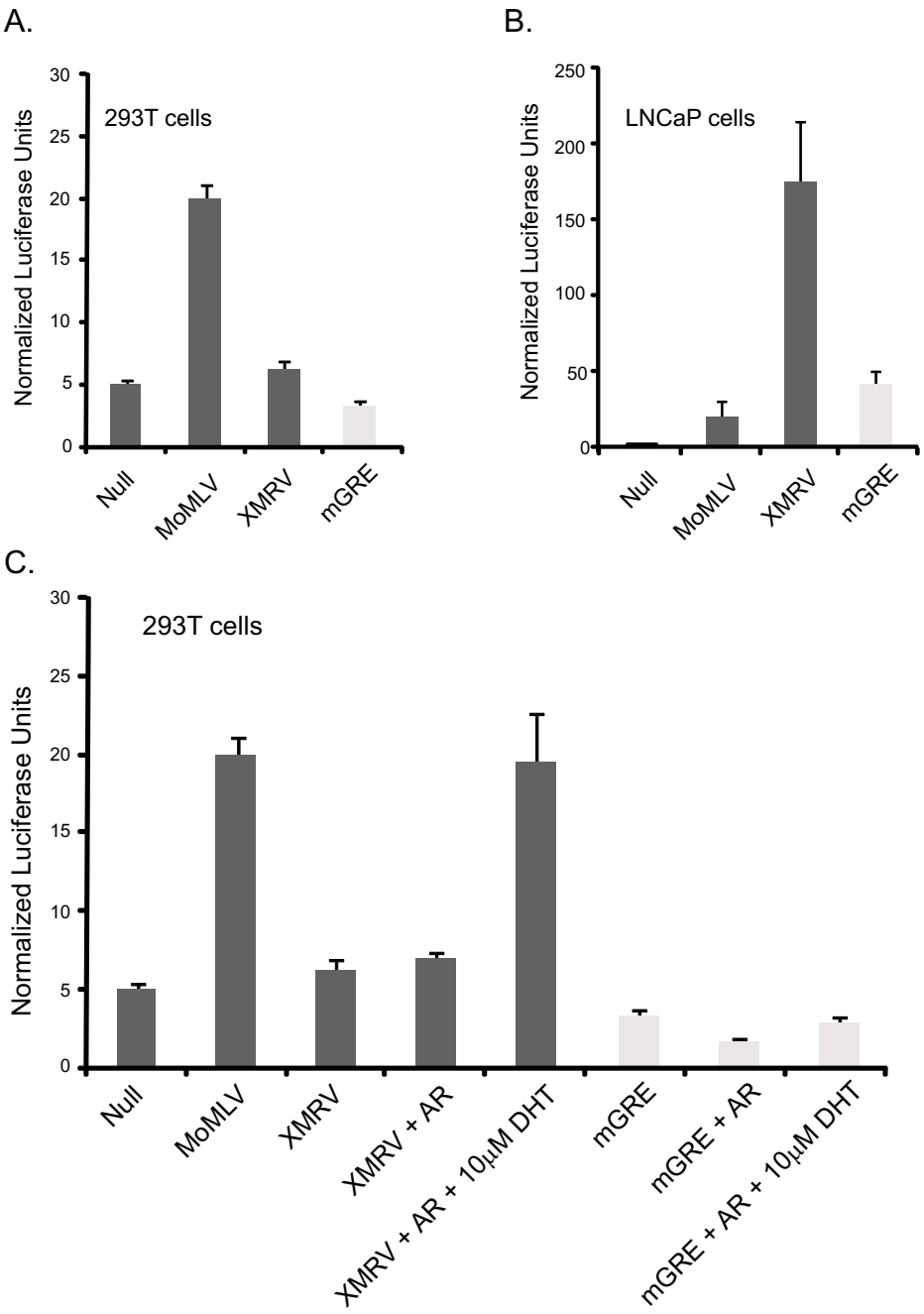
A.
293T cells
Normalized Luciferase Units
30
25
20
15
10
5
0
Null
MoMLV
XMRV
mGRE
B.
LNCaP cells
Normalized Luciferase Units
250
200
150
100
50
0
Null
MoMLV
XMRV
mGRE
C.
293T cells
Normalized Luciferase Units
30
25
20
15
10
5
0
Null
MoMLV
XMRV
XMRV + AR
XMRV + AR + 10μM DHT
mGRE
mGRE + AR
mGRE + AR + 10μM DHT